^{57}Fe Mössbauer Study of Tektites

B. J. Evans and L. K. Leung

Department of Chemistry
University of Michigan
Ann Arbor, MI 48109

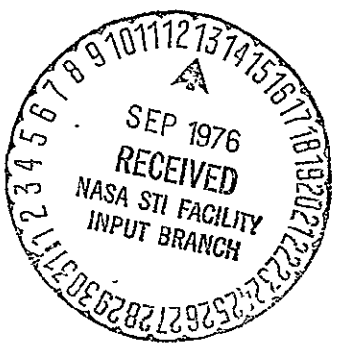

ABSTRACT

^{57}Fe Mössbauer measurements have been made selected moldavite, australite, philippinite and georgia tektites. The spectra consist of two apparent lines but at least two quadrupole doublets can be fitted to these spectra. The Mössbauer parameters for these doublets indicate that they arise from Fe^{2+} ions with local environments, which are relatively rich and relatively poor in calcium, respectively, similar to those in clinopyroxenes. No evidence for Fe^{3+}/Fe^{2+} ratios above 0.01 (estimated detection limit) have been found in any tektite. Tektites are considerably more reduced than previously believed and the extent of the reduction shows little or no variation among different types of tektites. These results limit the source materials of tektites to minerals in which the iron is uniformly highly reduced and in which the iron is contained clinopyroxene-like phases.

I. INTRODUCTION

The origin and source materials of tektites continue to be a conundrum. On the one hand, there is agreement among some investigators on their connascence with terrestrial meteoritic impact events while, on the other hand, there is a concensus among a smaller, more active group of tektite investigators that tektites are lunar materials being either the ejecta from a lunar meteoritic impact or lunar volcanism.[1]

In his recent monograph on tektites O'Keefe[1] has given a well-balanced review of the different theories on the origins of tektites and their strengths and shortcomings in the light of the experimental evidence. The experimental evidence on tektites most relevant to their origins is chemical in nature. Many physical properties measurements have been made on tektites but from among these, only the specific gravity determinations have provided unambiguous evidence in the study of the origin of tektites. However, for glasses it is possible to view the specific gravity as being primarily a chemical parameter except in those cases in which the glass has been subjected to high pressures.

Unfortunately, there are numerous accidental degeneracies in the chemical compositions of different kinds of rocks. Further difficulties are occasioned by the range of compositions within a possible rock type or material at a source site. The intrinsic difficulty with sourcing studies employing composition data, however, is that of using all of the available information. Linear plots, scattergrams and ternary plots are difficult to evaluate when the number of composition variables become as large as they

are for tektites and possible tektite source materials; and it is highly probable that a considerable amount of information is suppressed in these two and three-dimensional representations. A detailed account of defining source materials and some remedies to current techniques has been published recently.[2]

The present investigation was mounted as an application of modern theories of glass structure in determining the source materials and thermal histories of tektites. The idea that the local structure of a glass is similar to that of the crystalline material from which it was derived, with the similarities in local structures being influenced significantly by thermal history, was crucial to our research plan.[3] Immediately before and during the course of this study, it was shown that even SiO_2 and GeO_2 glasses have significant local order reminiscent of certain crystalline polymorphs.[4] Indeed, it has been shown that in aqueous glasses one needs cooling rates of greater than 10^4 K/sec to completely suppress significant local ordering and the formation of ultra-microcrystalline-like regions.[5] The higher viscosity of silicate melts is expected to lead to a significantly lower critical cooling rate, but systematic studies on the minimum cooling rate necessary to suppress the formation of ultra-microcrystalline-like regions in silicates are lacking. Our measurements do indicate, though, that the cooling rates for the tektites are not high enough to prevent the formation of ordered local regions in these glasses.

The systematics of the relationships between the Mössbauer parameters at 298 K and the chemical analyses indicate that the majority of the Fe^{2+} ions have local crystal/chemical structures

that are similar to those of the M1 site in clinopyroxenes.[6] Consistent with the metastable nature of glasses and the non-equilibrium atomic topology, the M1 sites appear to be more distorted in the glasses than in the crystals. Least squares fits of the spectra indicate the Fe^{2+} ions to occupy two predominate kinds of M1 sites. These two sites appear to be related to calcium-rich and calcium-poor regions in the glasses as has been found for C2/c crystalline clinopyroxenes.

Despite similarities in major element composition to other Australasian tektites, the HCuB tektite of Chapman and Scheiber[7] give quite different Mössbauer spectral parameters. This result is interpreted as evidence of differences in the thermal histories of these tektites relative to those of other chemical types in the Australasian field, as concluded by Chapman and Scheiber from trace elements analysis.

From measurements on tektite having wet chemical determination of the Fe^{3+}/Fe^{2+} ratio it is concluded that this ratio determined chemically is larger than the actual ratio: the Fe^{3+}/Fe^{2+} ratio in tektites is well below 0.05. The oxygen fugacity was extremely low during either the formation of the tektite source materials, at the time of tektite formation or both . For small Fe^{3+}/Fe^{2+} ratios in samples containing less than 10 weight percent total FeO, the Mössbauer resonance technique appears to offer optimal accuracy and precision.

Mössbauer spectra were also obtained for a visibly inhomogeneous Philippinite. Using a small-area sampling technique which has been proven on metamorphic rocks containing intermixed spinel-pyroxene

phases, there appeared to be no difference in either the amount or type of local structures associated with Fe in the dark and clear bands of this specimen. Either the dark bands (1) do not contain any micro-crystals, (2) do not contain iron-containing microcrystals, or (3) the amount of iron-containing microcrystals is below our detection limits. Scanning electron microscopy studies support either (1) or (2).

II. EXPERIMENTAL

II.1 Samples Provenance:

A total of twenty synthetic glass specimens, 31 analyzed tektites and 49 unanalyzed tektites were acquired for Fe^{57} Mössbauer measurements. The Fe^{57} Mössbauer spectra of all but three (Georgia tektites) of the analyzed tektites have been obtained at 298 K. These samples and their descriptions are listed in Table I. Fe^{57} Mössbauer spectra have also been obtained at 298 K for four of the tektites for which chemical analyses are not available. These specimens consist of two moldavites (NMNH 2222 and 2230), one Libyan Desert glass (NMNH 1212) and the Ortigas site specimen PO-1. The Fe^{57} Mössbauer spectra of two of the synthetic glass specimens have been obtained so far. One specimen was annealed for various time periods and at different temperatures and the Fe^{57} Mössbauer spectra obtained at 298 K in order to study crystallization and nucleation phenomena and the relationship of the local structure in the glass to that in the crystallization products.

Several unanalyzed Muong Nong tektites were cut into thin wafers in search for regions of marked inhomogeneities. Since no marked inhomogeneities relative to the other tektites were found, no Fe^{57} Mössbauer spectra were obtained for this type of tektite.

II. 2. Mössbauer Spectroscopy:

The Mössbauer spectrometer was of the constant acceleration, "flyback" type operated in "time-mode". To obtain high-resolution spectra, 512 channels of a 1024 channel analyses were used to record the data.

Of special significance to this study was the use of very small area sources, ∿1 mm in diameter, which made possible the collection of superior quality data. The sources used were either a 25 milliCurie Co^{57}/Rh or a 20 milliCurie Co^{57}/Cu source. Mössbauer spectra were obtained on sample areas less than 2 mm^2. The beam was well collimated by means of a 3/8"-thick graded shield with a 1.5 mm diameter aperture and a 2-in. long, adjustable slit collimator with typical aperture dimensions of 1 mm x 1 mm. The collimators were found to be essential to obtaining reproducible results at high precision.

All Mössbauer absorber specimens were in the form of thin, ∿1 mm thick, wafers. The sample handling technique precluded the possibility of oxidation and other chemical and structural changes that might accompany any grinding or powdering of the specimen. The absorber thickness was less than 7.2 mg of natural Fe per cm^2.

The spectrometer was calibrated after each set of three or four runs using a 0.013 mm thick Fe metal foil and a commercially available sodium nitroprusside standard absorber. The zero velocity channel was determined using a Co^{57}/Fe source and the above-mentioned Fe metal absorber. The velocity increment per channel for all of the tektite spectra was approximately 0.01 mm/sec per channel. The width of the innermost lines of the Fe metal foil and the sodium nitroprusside absorbers was 0.29 mm/sec. Because of the strong collimation of the γ-ray beam, geometrical broadening of the lines and shifts in line positions are negligible. The linewidths of the Fe metal and sodium nitroprusside absorbers obtained with the 25 milliCurie Co^{57}/Rh source are larger than those of 0.22 mm/sec obtained under similar conditions with a 10 milliCurie Co^{57}/Cu having an active area of 36 mm^2. The larger linewidth for the Co^{57}/Rh source is due primarily to its high activity; the linewidth of the Fe metal foil and sodium nitroprusside obtained with the 25 mCi Co^{57}/Rh source is, however, smaller than the intrinsic linewidths of crystalline silicates and no loss in resolution is incurred.

All experiments were performed on a 2000-kilogram air-cushioned, vibration-isolated table. The Mössbauer motor, absorber, and detector were mounted on a lathe-bed optical bench, thereby insuring precise and reproducible alignment of the various components. For the small-area measurements on the Ortigas site specimen a precision, X-Y-Z micrometer translator with an accuracy and resettability of 0.01 mm was used to position the desired region of the specimen in the γ-ray beam.

A vacuum insulated glass dewar was used to obtain the Mössbauer spectra at liquid nitrogen temperature. The sample was cooled by conduction via a massive copper sample block which was in direct contact with the cryogenic fluid. The dewar was mounted vertically with the direction of propagation of the γ-rays being horizontal and perpendicular to dewar axis. The geometry was similar to that used in the room temperature measurements, except for a larger source-counter separation.

The Mössbauer spectral parameters were derived from computer-assisted least-mean-squares fits of Lorentzian shaped lines to the spectrum. Any line shape that can be expressed in closed form, however, can be fitted to the spectra. In addition to the usual chi-square goodness-of-fit criterion given by the equation below

$$\chi^2 = \sum [N(i)_{calc} - N(i)_{exptl}) / \sqrt{N(i)_{exptl}}]^2$$

where i refers to data point i (or velocity v_i); $N(i)_{Exptl}$ is the experimental number of counts at velocity i; $N(i)_{Calc}$ is the calculated number of counts at velocity i determined from the least-mean-squares fit; and p is the number of data points; a newly developed and much improved goodness-of-fit parameter has also been used. This parameter, known at this time as "MISFIT", provides one with a simultaneous measure of the quality of the experimental data and the agreement between the fitted spectrum and the experimental data.[8] The usual χ^2 parameter does not permit one to determine if a given data set is of high

enough quality to adequately test the validity of one's model. MISFIT has proven to be particularly useful in providing insights into the number of sites occupied by Fe^{2+} and the existence of structural inhomogeneities in our small-area studies.

III. RESULTS

Typical Fe^{57} Mössbauer spectra obtained at 298 K of tektites from the various strewn fields are given in Figs. 1, 2, 3, 4, and 5. The diamond points are the experimental data and the lines, showing both the individual components and their envelopes, are the results of fitting two Lorentzian shaped lines to these spectra. The widths, intensities and positions of each line were allowed to vary independently. These were, therefore, eight parameter fits: six variable parameters for the two lines and two parameters for the non-resonant variation in count rate. This variation is parabolic as a result of the strong collimation and relatively large stroke amplitudes of the velocity transducer.

The normalized difference between the experimental spectrum and the fitted spectrum, called the RESIDUAL, is also plotted. For an adequate fit, the RESIDUAL, which is given by the relationship

$$\text{RESIDUAL}(i) = [(N(i)_{\text{Calc}} - N(i)_{\text{Exptl}})]/\sqrt{N(i)_{\text{Exptl}}} \quad ,$$

should have a maximum amplitude of ±1 and be completely random, i.e., like "grass" over the entire velocity range as shown in Fig. 6. Using the criteria of the absence of structure in the RESIDUAL and a small χ^2 ($\sim$500), the two-line fits to the

tektite spectra, of which Fig. 5 is typical, are clearly inadequate. Alternate fits and their implications will be discussed in a later section.

Nonetheless, our fits to all of the tektite spectra resulted in RESIDUALS that are qualitatively quite similar and of approximately the same magnitude, and the parameters of the two line fits can be used as a basis for our initial discussions. Similarities and differences in the spectral parameters for different specimens will have definite relative significance. The parameters resulting from the two line fits are listed in Tables 2 and 3.

III. 1. Reconnaissance Measurements:

As shown in Table 2, the Mössbauer parameters are not unique for a given tektite type and it does not appear likely that Mössbauer parameters can be used to reliably distinguish among tektites from different strewn fields, contrary to the suggestions of an earlier study.[9] However, what correlations do exist between the Mössbauer spectral parameters of tektites in the same strewn field have, as shall be shown later, geochemical and local structural bases which extend across different strewn fields.

III. 2. Selected Area Measurements on the Ortigas Site Philippinite Specimen

The spectra for the Ortigas site specimen (Fig. 7) obtained on and off of the dark bands are shown in Figs. 8 and 9. The parameters resulting from two line fits are given in Table 4.

It is clear from Table 5 and the spectra themselves that there is no detectable difference in the nature of the Fe^{2+} species in the dark and light bands. Another spectrum was obtained with the longer collimator and the χ^2 of the two-line fit to this spectrum (cf. Table 5) is quite different from those obtained with the short collimator (cf. Fig. 2). However, the counts per channel are different for the two sets of spectra and the χ^2 goodness-of-fit parameter is unsuitable for comparison purposes. Therefore, we have used the MISFIT goodness-of-fit parameter[8]--along with its associated parameters SIGNAL and DISTANCE -- in analyzing these data. These results are given in Table 5.

SIGNAL is a measure of the quality of the data and is proportional to the percent absorption of the line, the number of counts per channel, and the number of channels used to record the spectrum, e.g., those channels associated with possible resonance absorption lines and is given by the following relationship

$$\text{SIGNAL} = \sqrt{\sum_{i=1}^{p} \left[\left(\frac{N(i)_o - N(i)}{\sqrt{N(i)}} \right)^2 - 1 \right]} .$$

where $N(i)_0$ is the number of counts that would be in channel $\underline{i}$ if there was no absorber and N(i) is the actual number of counts in channel $\underline{i}$, i.e., with the absorber present, and p is the number of data points. For the geometry employed in our tektite studies $N(i)_0$ has a parabolic dependence on velocity and is given by

$$N(i)_0 = N(0)_0 \ (1 \pm \alpha \ V(i)^2)$$

$N(0)_o$ is the number of counts either at zero velocity; α is a constant dependent upon the source absorber-detector geometry, and V(i) is the velocity at data point i. As the quality of the data improves, SIGNAL increases; typically SIGNAL should be $\sim 10^7$.

DISTANCE is defined as

$$\text{DISTANCE} = \sum_{i}^{P} (X^2(i)-1)$$

and is a measure of the agreement between the calculated and experimental spectra. MISFIT is defined as the ratio of DISTANCE to SIGNAL, i.e.,

$$\text{MISFIT} = \text{DISTANCE}/\text{SIGNAL}$$

A small value for MISFIT of the order of 0.1% or less indicates a good fit. It is necessary, however, that the standard deviation of MISFIT also be small -- much smaller than MISFIT itself for a given fit to a spectrum to be unique. A large value of MISFIT or a small value of MISFIT with a large standard deviation indicates that other fits to the data would be equally satisfactory. In this case, the data would not be of high enough quality to test the assumptions involved in the fitting models.

Returning now to the Ortigas site specimen, the values of DISTANCE, SIGNAL and MISFIT are given in Table 5. First of all, it is immediately clear that our two-line fit to the spectra are no worse for spectra taken on the dark bands than they are off of the dark bands. Thus, there are no spectral features associated with the dark bands of this sample that are different

from those associated with the light bands. Similarly, the difference in χ^2 for the spectra obtained with the different collimators is also seen to be non-diagnostic; the MISFIT values are quite similar despite the more than a factor of two difference in χ^2 .

III. 3. Synthetic Basalt Glass With "Known" Fe^{3+}/Fe^{2+} Ratio:

A sample of a synthetic basalt glass obtained from Corning Glass Works,[10] having a Fe^{3+}/Fe^{2+} ratio of 0.25 (9.1% Fe), 2.6% Fe_2O_3) exhibited the Mössbauer spectrum shown in Fig. 10 at 298 K. The presence of Fe^{3+} is clearly indicated by the shoulder on the high velocity side of the low velocity component of the Fe^{2+} pattern. The spectrum was fitted to two quadrupole doublets, one for the Fe^{2+} pattern and one for the Fe^{3+} pattern, and the resulting parameters are given in Table 6.

Outstanding among the results of these data analyses is the low value for the Fe^{3+}/Fe^{2+} ratio obtained from our Mössbauer measurements relative to the one derived from the wet chemical analyses. If errors of this magnitude can occur in the wet chemical analysis for these amounts of Fe^{3+} and Fe^{2+} ions, considerably larger relative errors are likely to occur for much smaller amounts of total Fe and lower Fe^{3+}/Fe^{2+} ratios such as in the case of tektites. Sample handling errors in our Mössbauer measurements are not likely. The specimen was used as a wafer; and the effects of surface oxidation (or reduction -- which need not be given serious consideration) if present would be negligible. It is noted that oxidation would improve the agreement between the

Mössbauer and chemical determination of the Fe^{3+}/Fe^{2+} ratio. There is now a substantial body of data to indicate that ^{57}Fe Mössbauer determinations of Fe^{3+}/Fe^{2+} ratios in silicates are more reliable and precise than wet chemical methods.[11] It is noteworthy that when there are differences between Fe^{3+}/Fe^{2+} ratios obtained by wet chemical and Mössbauer spectroscopic methods; the ratio is always larger for the wet chemical determination.

To gain some insight into possible saturation effects in the intensity of the absorption patterns which could greatly affect our derived Fe^{3+}/Fe^{2+} ratios, a portion of the basalt glass was ground under acetone into a fine powder and absorber discs of various thicknesses from 0.50 mg/cm^2 to 2.9 mg/cm^2 of natural iron were prepared. It is to be noted, however, that corrections for saturation effects cannot improve the agreement between the chemical and Mössbauer determinations of Fe^{3+}/Fe^{2+} since the Fe^{2+} pattern is expected to show saturation effects more strongly than the weaker Fe^{3+} spectrum. A linear dependence of the intensity of the patterns on the thickness of the sample and the constancy of the line widths indicated that saturation effects are nil. There was evidence of some oxidation during the grinding of the sample, however, inasmuch as the Fe^{3+}/Fe^{2+} area ratio increased from 0.126 for the wafer to 0.167 for the powders. If any of the tektites were ground prior to chemical analysis, the Fe^{3+}/Fe^{2+} ratio is sure to be higher than that in virgin specimens Contrary to the previous conclusion regarding the reliability of Fe^{3+}/Fe^{2+} determinations in glasses,[9] it is our opinion that

Mössbauer spectroscopy provides an optimal means for determining the Fe^{3+}/Fe^{2+} ratios, especially for small values of this ratio and small total iron content.

While the Mössbauer parameters of the Fe^{2+} ion for the synthetic basalt glass are similar to those for the tektites, this glass can be easily distinguished from the tektite by its rather different absolute and relative linewidths, i.e., Γ_{Low}, Γ_{High}, and $\Gamma_{Low}/\Gamma_{High}$ have typical values of 0.70 mm/sec, 0.90 mm/sec, and 0.80, respectively, for tektites, whereas for the basalt glass these values are 0.70 mm/sec, 0.80 mm/sec, and 0.85, respectively: The asymmetry of the Fe^{2+} spectrum in the basalt is not as great as that in the tektites.

III. 4. Libyan Desert Glass:

One sample of Libyan Desert glass was kindly provided by Roy Clarke, Jr., of the National Museum of Natural History, Meteorite Division. The sample, NMNH 1212, had numerous bubbles and was very pale yellow in color. There was little indication of there being even 1% FeO in this glass as has been reported for another Libyan Desert glass specimen.[12]

The ^{57}Mössbauer spectrum of this specimen is shown in Figure 11. There is certainly very little iron in this specimen and the iron content is well below 1%. While the evidence for absorption peaks in the spectrum is very tenuous, the presence of very weak absorptions are obvious in the plot of the difference between a fit to a non-resonant curve and the experimental data, e.g., the

RESIDUAL plot below the spectrum. The RESIDUAL in this case is identical to SIGNAL. If there were no absorption peaks, SIGNAL would have been equal to zero. The value observed for SIGNAL is 262. This is to be compared with a typical value of $10^6 - 10^7$ for SIGNAL for the Australasian tektites.

The two weak absorption peaks appear to have the same characteristics of positions, relative widths, and intensities as other tektites but a definitive comparison cannot be made.

III. 5. Low-Temperature Measurements on Specimen AN216

This specimen is designated as a HCa type by Chapman and Scheiber.[7] Even though the CaO/MgO ratio is greater than 1 for this specimen, the CaO content is only 2.35 weight percent and is nearly equal to that in other tektites that are not classified as HCa. Neither are the Mössbauer parameters of this specimen consistent with its having unique type (cf. Tables 1 and 2) local structures. Apparently, the Mössbauer parameters are more sensitive to the absolute amount of CaO than to its content relative to some other element. This result has important implications for the local environment of Fe^{2+} in tektite glasses.

The Mössbauer spectrum of this specimen (Fig. 12) exhibited a weak shoulder on the high velocity side of the high velocity peak which prompted us to make further measurements at liquid nitrogen temperatures. The plot of the residual in Fig. 12 resulting from our usual two line fit clearly shows the presence of this weak absorption. The parameters of a single quadrupole doublet and a two quadrupole doublet fit are shown in Table 7.

At liquid nitrogen temperatures, the presence of more than one quadrupole doublet pattern is obvious, Fig. 13. The results of fitting the liquid nitrogen spectrum to a single quadrupole doublet and to two quadrupole doublets are also shown in Table 7. Clearly, the two quadrupole doublet fits adequately describe the data at both temperatures; the single quadrupole doublet fails to account for the data. The consistency of the two quadrupole doublets fits at the two temperatures is also encouraging. Furthermore, even though the structure in the RESIDUAL would indicate the presence of other absorption lines, it is clear from the value of MISFIT that the data could not be used to adequately test the assumptions of such a model. The parameters obtained from the fit of two quadrupole doublets are very similar to those of crystalline pyroxenes, especially the C2/c clinopyroxenes.[6]

III. 6. Mössbauer Spectra of Crystalline Pyroxenes:

The room temperature Mössbauer spectra of two crystalline pyroxenes were obtained for the purpose of comparison with the spectra of the glasses. Two specimens, a bronzite of composition $Mg_{1.445}Fe_{.427}{}^{-Al}{}_{.157}Si_2O_6$ and a clinopyroxene of composition $Ca_{.86}Mg_{.58}Fe_{.52}Si_2O_6$ were studied.[13] The bronzite was studied in order to check the reliability of our fitting techniques; and the clinopyroxene was studied in order to provide substantive insights into the nature of the Fe^{2+} sites in the tektite glasses.

The results of various alternative fits to the data are given in Table 8. The single quadrupole doublet fits are employed simply to indicate the motivation for the more complex fits. The fit of two quadrupole doublets to the bronzite spectrum

is adequate and the parameters are very similar to those obtained by other workers for pyroxenes of similar composition.[14] The anomalies noted previously[10] in the relative intensities of the two quadrupole doublet fits to the Fe^{57} Mossbauer spectra of clinopyroxenes at 298 K are not observed in our fits. The pattern assigned to the M1 site is the more intense one, as expected. While a three quadrupole doublet fits leads to a smaller χ^2, the relative intensities of the patterns are inconsistent with the crystal chemistry of the pyroxene and MISFIT is actually larger. The three line fit does not appear to have any physical significance in terms of our present knowledge of the structures of clinopyroxenes.[6] There seems to be little point, therefore, in attempting to fit more than two Fe^{2+} patterns to the tektite spectra.

From the nature of the residuals of these measurements, we have some basis for fitting the tektite spectra to more complex patterns. For example, the existence of four peaks in the residual, with two pair associated with each peak, implies that only two absorption peaks have been neglected in the fitting model, etc.

IV. DISCUSSION

In Fig. 14, the variation in ^{57}Fe isomer shift of the samples in Table 1 with quadrupole splitting is plotted. There is a positive correlation between the two quantities for the Australasian tektites. This result is very similar to that observed in crystalline Fe^{2+} compounds in which the near neighbor atoms of an Fe^{2+} ion are varying in type and quantity in a systematic

fashion.[15] Hence, the lattice sites occupied by the Fe^{2+} ion in tektite glasses are not random or of a great multiplicity of types. Furthermore, what variations exist in the topology and chemical bonding at these sites are also of a systematic nature.

In addition, the magnitude of the quadupole splitting shows a general tendency to decrease with increasing calcium content, as shown in Fig. 15. Neither the quadrupole splitting nor isomer shift exhibit a regular variation with respect to the concentration of any other major element. Herein resides a clue as to the kind of site occupied by the Fe^{2+} ion. In Figs. 16 and 17 the variations in the quadrupole splitting with calcium content for the M1 and M2 sites in the hedenbergite-ferrosilite solid solution series and of the M1 and M2 sites of the enstatite-ferrosilite solid solution series, respectively, are presented. The dependence of the Fe^{2+} quadrupole splitting on calcium content in the tektites is similar to that of the M1 Fe^{2+} ions in the clinopyroxenes. A similar relationship also exists between the tektites and pyroxenes along the diopside-hedenbergite join as shown in Fig. 18. Indeed, the magnitude of the Fe^{2+} quadrupole splitting in the diopside-hedenbergite solid solution series is very similar to those in the tektite glasses. These results suggests that the iron sites in tektites have local structures that are rich in calcium. Since both the calcium and iron contents of the tektites are rather low, close associations between Fe and Ca are not expected in a completely random glass and the existence of Fe-Ca clustering is likely to be due to vestigial, local, atomic arrangements of the source material, strongly implicating calcium rich clinopyroxenes as among the tektite source material.

Orthopyroxenes cannot be ruled out as being among the possible source materials of the Australasian tektites; but the systematics of the available evidence favor the clinopyroxenes.

There are some exceptions to the correlations and notable among these is the HCuB tektites, cf. Fig. 14. This deviation can be interpreted as resulting from different thermal histories for the HCuB tektites in relation to other Australasian tektites. A similar conclusion has also been reached on the basis of trace element abundances by Chapman and Scheiber.[7] Further studies on additional HCuB tektites are required to substantiate the proposed milder heating of these tektites. The moldavites and Georgia tektites studies also provide insights into the differences between other tektites and the Australasian tektites. If the HCuB tektites were less severely heated than other Australasian tektites, then the Georgia tektites and modavites were more severely heated than the Australasian tektites.

Without exception for the specimens studied so far, the estimates of the Fe^{3+}/Fe^{2+} ratios seem to be much too high. The highest reported Fe^{3+}/Fe^{2+} ratio of the specimens we have studied is 0.1223 for a Georgia tektite NMNH 1396 (cf. Fig. 6).[16] From our measurements on the synthetic basalt glass, it is clear that the Fe^{3+} content of this Georgia tektite is considerably smaller than the above ratio.

For very small amounts of Fe^{3+} as expected in tektites, it is possible that the weak Fe^{3+} absorption observed in the synthetic basalt would degenerate either into a broadening of the low velocity

Fe^{2+} line or an increase in the relative integrated intensity, i.e., area of the low velocity line. Neither of these expectations is borne-out by the data. As shown in Fig. 18, the difference between the widths of the high and low velocity lines, $\Gamma_H - \Gamma_L$, of 0.172 mm/sec for the Georgia tektite NMNH 1396 is not much smaller than that of other tektites. In particular $\Gamma_H - \Gamma_L$ of 0.166 mm/sec for the Georgia tektite NMNH 2343 is smaller than that of NMNH 1396. The Fe^{3+}/Fe^{2+} ratio of specimen 2343, determined by wet chemical analyses, is <0.001. A similar conclusion is reached from a consideration of the relative areas of the high and low velocity lines. The larger the ratio of A_{Low}/A_{High}, the stronger the indication of the presence of Fe^{3+}. One of the highest vales of A_{Low}/A_{High} (1.007) shown in Fig. 19 is for Georgia tektites NMNH 2345. The Fe^{3+}/Fe^{2+} ratio determined by wet chemical methods for this specimen is 0.0173. The value of A_{Low}/A_{High} for NMNH 1396 is 0.991. No evidence can be found to support the presence of Fe^{3+} ions within the detection limits of the Fe^{57} Mössbauer effect.

There is little to discuss with respect to the bands and the existence of microcrystals in the Ortigas site specimen. There do not appear to be any Fe-containing microcrystals in the dark bands. Unless previous investigators[17] are willing to propose that there can be other kinds of microcrystalline inclusions in the Ortigas site specimens, the interpretation of the magnetic properties of these tektites should be reconsidered.

The low-temperature measurements on specimen AN216 are quite revealing. In this specimen there are at least two kinds of sites

for the Fe^{2+} ion. There appear however to be no more than three kinds of sites that occur in significant numbers. The possibility of a third very weak doublet pattern is indicated in the RESIDUAL of the fit of two doublets (Fig. 13); but there is a need for further study to firm-up this possibility. Again, the similarity of the Fe^{2+} sites in the tektites to those in the clinopyroxenes is indicated by the low temperature measurements. The magnitudes of the quadrupole splittings are very similar to those in a pyroxene of approximate composition $Ca_{.8}Fe_{.6}Mg_{.6}Si_2O_6$.[4] There are still some questions regarding the relative intensities of the two patterns and hence the frequency of occurrence of the two kinds of sites, but it is not expected that all of the details of the local structure of the crystalline phases would be maintained in the glasses.

Finally, the weak temperature dependence of the quadrupole splitting and the smaller isomer shift of the Fe^{2+} ions relative to that observed for 6-coordinated ferrous ions in crystalline phases are consistent with our conclusions on the local structure of the Fe^{2+} sites in tektites and can be understood as resulting from the somewhat greater distortions of the $Fe\text{-}O_6$ polyhedra and increased covalency of the Fe-O bonds in the glass. It has been suggested on rather general grounds that the covalence of metal-oxygen bonds increase on going from the crystalline to the glassy state[18] and our results are consistent with these suggestions.

V. CONCLUSION

Of the above results those bearing most directly on the question of the origin of Tektites are: (1) the observation of local Fe^{2+} environments similar to those in clinopyroxenes; (2) the low Fe^{3+} content and (3) the failure of the HCuB tektites to fit into the systematics exhibited by other tektites. It would be indiscrete to claim that these results can lead directly to a knowledge of the source materials and source sites of tektites. They do serve, however, to place unambiguous restraints on source materials and to a lesser extent on source sites. In the framework of modern theories of glass structure, clinopyroxenes are clearly implicated as being among the phases present in tektite source materials and any proposed rock type must contain this mineral.

It is common knowledge and universally accepted that tektites are highly reduced. However, Fe^{3+}/Fe^{2+} ratios as high as 0.1 and an approximately average value of 0.05 have been reported. Our results indicate that the Fe^{3+}/Fe^{2+} ratio is much less than 0.1, even for those samples having wet chemical Fe^{3+}/Fe^{2+} values greater than 0.1. Indeed, if we use the area ratio of the low velocity peak to the high velocity peak as a measure of the Fe^{3+}/Fe^{2+} ratio, then our spectra indicate a negative value for the Fe^{3+}/Fe^{2+} ratio. That is to say, when the area ratio A_{Low}/A_{High} is greater than one then Fe^{3+} is present; if the ratio is equal to one, then no Fe^{3+} is present; and if the ratio is less than one, then the physically unacceptable result that the Fe^{3+} content is less than zero

is obtained. Thus, the Fe^{3+} content is very low - much lower than 0.05 and lies in a range that cannot be obtained by the high temperature fusion of terrestrial rocks. ^{57}Fe Mössbauer measurements have been performed on several impactite specimens from the Ries Crater, Bosumtui Crater and Darwin glass and all of these contain appreciable amounts of Fe^{3+} ions.

The results of our measurements on the HCuB sample are significant since we find this sample to be unique with our measurement technique in agreement with trace element analysis even though the two different measurements are quite independent of each other. Further measurements on such samples might lead to more information concerning the thermal history of tektites and serve to further delimit the possible source materials, source site and formation processes.

ACKNOWLEDGEMENTS

Support of this research by NASA Grant NGR-23-005-537 is gratefully acknowledged.

REFERENCES

1. O'Keefe, J. A., Tektites and Their Origin, 254 pp., Elsevier, New York, 1976 and references therein.
2. Ward, G. K., A Systematic Approach to the Definition of Sources of Raw Material, Archaeometry 16, 41-53 (1974).
3. Zarzycki, J., X-Ray Diffraction of Alkali Titanate Glasses, J. Mater. Sci. 6, 130-135 (1971);
   Leadbetter, A. J. and Wright, A.C., Diffraction Studies of Glass Structure I. Theory and Quasi-Crystalline Model, J. Noncryst. Solids 7, 23 - (1972).
   Leadbetter, A. J. and Wright, A. C., Diffraction Studies of Glass Structure II. The Structure of Vitreous Germania, J. Noncryst. Solids 7, 37 - (1972).
4. Ferguson, G. A. and Hass, M. , Neutron Diffraction Investigation of Vitreous Germania, J. Amer. Ceram. Soc. 53, 109-111 (1971).
   Konnert, J. H., Karbe, J., and Ferguson, G. A., Crystalline Ordering in Silica and Germania Glasses, Science 179, 177-179 (1976).
5. Cohen, R. L. and West, K.W., Mössbäuer Spectroscopy of Frozen Solutions, Chem. Phys. Letters 13, 482 - 484 (1972).
6. Williams, P. G. L., Bancroft, G. M., Brown, M. G., and Turnock, A. C., Anomalous Mossbauerspectra of C2/c Clinopyroxenes, Nature 230, 149 - 151 (1971).
7. Chapman, D. R. and Scheiber, L. C., Chemical Investigation of Australasian Tektites, J. Geophys. Res. 74, 6737 - 6776 (1969).

8. Ruby, S. L., Why MisFit When you have χ^2? in Mossbauer Effect Methodology, Vol. 8, edited by I. J. Gruverman and C. W. Seidel, 263 - 276, Plenum Press, New York, 1973.

9. Marzolf, J. G., Dehn, J. T., and Salmon, J. F., Mossbauer Studies of Tektites, Pyroxenes and Olivines in the Mossbauer Effect and Its Application in Chemistry edited by R. F. Gould, 61 - 85, American Chemical Society, Washington, D. C., 1967.

10. Kindly supplied by Robert H. Dalton of Corning Glass Works, Sullivan Park, Corning, New York.

11. Haggstrom, L., Wappling, R., and Annersten, H., Mossbauer Study of Oxidized Iron Silicate Minerals, Phys. Stat. Sol. 33, 741 - 748 (1969).

Frischat, G. H., Zellerfeld, C., and Tomandl, G., Mossbauer Investigation of Silicate and Phosphate Glasses with Small Additions of Fe_2O_3, Glastechn. Ber. 44, 173-177 (1971).

Hafner, S. S., Mossbauer Spectroscopy in Lunar Geology and Mineralogy in Topics in Applied Physics, Vol. 5 (Mossbauer Spectroscopy), edited by U. Gonser, 167 - 197, Springer-Verlag, New York, 1976.

12. Baker, G., Tektites in Mem. Nat. Mus. Vict. 23, 313 pp., National Museum of Victoria, Melbourne, 1959.

13. Kindly supplied by D. Virgo of the Geophysical Laboratory, Washington, D. C.

14. Bancroft, G. M., Williams, P.G.L. and Burns, R. G., Mossbauer Spectra of Minerals Along the Diopside Hedenbergite Tie Line, Amer. Min. 56, 1617 - 1625 (1971).

15. Hazony, Y., H_c-QS-IS Correlations in Octahedral Iron Compounds in Mossbauer Effect Methodology, Vol. 7, edited by I. J. Gruverman, 147-166, Plenum Press, New York, 1971.

16. Cuttitta, F., Clarke, Jr., R. S., Carron, M.K., and Annell, C. S., Martha's Vineyard and Selected Georgia Tektites: New Chemical Data, J. Geophys. Res. 72, 1343-1349 (1967).

17. Thorpe, A.N. and Senftle, F. E., Submicroscopic Spherules and Color of Tektites, Geochim. et Cosmochim. Acta 28, 981-994 (1964).

18. Evans, B. J., Unpublished Results, 1975-76.

Table 1. Chemical Compositions of Tektites Studied

Sample Number	Description	Chemical Type	Major Element Analyses (Weight %)						
			Al_2O_3	FeO	MgO	CaO	Na_2O	K_2O	TiO_2
P-442	Kubao, Rizal, Phil.	HCa	12.5	4.83	2.59	7.77	1.06	2.06	0.68
NMNH-2230	Habri, Bohemia, Czech.								
AN-273	Mt. Davies, So. Aust	NA(?)	12.6	5.25	2.97	4.41	1.17	2.14	0.73
AN-274	Bulgara Hill, So. Aust		10.1	3.73	1.43	1.92	1.05	1.97	--
AN-216	Billakallina, So. Aust.	HCa	11.1	4.20	1.66	2.35	1.13	2.21	0.75
AN-272	Raspberry Bore, So. Aust	HCa?	10.3	3.69	1.44	2.23	1.13	2.12	0.58
P-215	Paracale, Bikol, Phil,	NP	12.2	4.65	2.07	2.65	1.51	2.60	0.78
AN-222	Cue, West Aust.	NA	13.3	4.54	2.19	3.09	1.53	2.57	0.78
AN-13	Kulin, West. Aust.	NA	12.7	4.65	2.15	2.90	1.22	2.32	0.76
AN-125	Ethawarra Waterhole, So. Aust	HCa	9.6	3.81	1.43	2.52	1.10	2.09	0.58
AN-214	Boyce Ck., West Aust.	NA	13.8	4.69	2.23	3.50	1.40	2.33	0.78
J-35	Sangiran, Java	HMg	10.8	5.55	3.65	2.21	1.14	2.09	0.69
P-461	Bulasa, Argao, Cebu	NP	13.6	4.85	2.25	2.98	1.48	2.58	--
T-220DK	Ubol, Thailand	HCuHB	13.4	4.85	2.27	2.86	1.69	2.70	0.87
I-63	Pakse, Laos	HCuHB	14.1	4.88	2.02	1.67	1.56	2.84	0.95
I-43	Pia Oac, N. Vietnam	NI(?)	13.5	4.47	2.04	2.41	1.17	2.40	0.72
T-191	Kasetsomboom, Thailand	NI	13.1	4.49	2.00	2.17	1.27	2.36	0.88
NMNH-2222	Dukovany, Moravia, Czech.								
Po-1	Ortigas, Phil.								
P-386	Echaque, Isabela, Phil.	LCaHA2	16.4	5.41	2.56	1.94	1.31	2.67	0.92
P-195	Pagranayan-Santiago, Phil,	LCaHA2	16.4	5.75	2.96	1.82	1.08	2.52	0.92
P-344	Echaque, Isabela, Phil.	LCaHA2	16.8	5.78	2.84	1.87	1.05	2.52	0.83
NMNH-2345	Georgia		10.6	2.30	0.57	0.51	1.12	2.51	0.48
NMNH-2343	Georgia		11.3	2.88	0.62	0.51	1.17	2.36	0.50
NMNH-1396	Georgia		11.4	2.53	0.61	0.63	1.21	2.34	0.52

Table 2. Fe^{57} Moessbauer Spectral Parameters of Tektites at 298 K

Sample Number	Linewidth Γ_L (mm/s)	Linewidth Γ_H (mm/sec)	Isomer Shift w.r.t. Fe (mm/s)	Quadrupole Splitting (mm/s)
P-442	0.674±0.013	0.873±0.014	1.041±0.002	1.880±0.005
NMNH-2230	0.663±0.007	0.886±0.008	1.052	1.813
AN-273	0.721±0.002	0.899±0.005	1.064	1.931
AN-274	0.722±0.013	0.921±0.012	1.064	1.909
AN-216	0.741±0.007	0.938±0.007	1.064	1.934
AN-272	0.711±0.006	0.923±0.006	1.065	1.912
P-215	0.735±0.003	0.934±0.005	1.065	1.940
AN-222	0.730±0.004	0.922±0.004	1.065	1.933
AN-13	0.724±0.006	0.917±0.006	1.067	1.935
AN-125	0.712±0.001	0.905±0.006	1.068	1.900
AN-214	0.730±0.005	0.931±0.005	1.069	1.941
J-35	0.720±0.005	0.901±0.005	1.071	1.951
P-461	0.718±0.001	0.922±0.004	1.072	1.953
T-220DK	0.737±0.004	0.908±0.004	1.073	1.996
I-63	0.738±0.008	0.919±0.008	1.074	2.025
I-43	0.715±0.004	0.895±0.003	1.081	1.955
T-191	0.724±0.004	0.918±0.004	1.085	2.005
NMNH-2222	0.722±0.007	0.936±0.006	1.089	1.951
Po-1 Band	0.725±0.007	0.921±0.007	1.091	2.039
Po-1 Clear	0.729±0.006	0.925±0.007	1.092	2.036
P-386	0.717±0.007	0.930±0.008	1.091	2.018
P-195	0.713±0.003	0.915±0.003	1.094	2.021
P-344	0.725±0.004	0.925±0.008	1.095	2.031
NMNH-2345	0.758±0.008	0.943±0.003	1.104	2.015
NMNH-2343	0.768±0.011	0.934±0.006	1.104	2.033
NMNH-1396	0.758±0.007	0.930±0.005	1.107	2.035

Table 3.

Area Ratios and Relative Linewidth Parameters of Fe^{57} Moessbauer Spectra of Tektites at 298 K

Sample Number	$\frac{Area_{Low\ Vel.}}{Area_{High\ Vel.}}$	$\frac{\Gamma_H-\Gamma_L}{\Gamma_H}$	$\Gamma_H(\Gamma_H-\Gamma_L)$ (mm^2/sec^2)	$\Gamma_H-\Gamma_L$ (mm/sec)	Γ_L/Γ_H
P-442	0.951	0.231	0.174	0.199	0.772
NMNH-2230	0.982	0.252	0.197	0.223	0.749
AN-273	0.966	0.198	0.160	0.178	0.802
AN-274	0.981	0.216	0.183	0.199	0.784
AN-216	0.979	0.210	0.185	0.197	0.790
AN-272	0.955	0.230	0.192	0.212	0.770
P-215	0.984	0.213	0.186	0.199	0.787
AN-222	0.986	0.209	0.177	0.192	0.792
AN-13	0.985	0.210	0.177	0.193	0.790
AN-125	1.025	0.213	0.194	0.193	0.787
AN-214	0.971	0.216	0.187	0.201	0.784
J-35	0.971	0.200	0.162	0.181	0.799
P-461	0.959	0.221	0.189	0.204	0.779
T-220DK	0.987	0.189	0.156	0.171	0.817
I-63	0.987	0.196	0.166	0.181	0.803
I-43	1.023	0.201	0.183	0.180	0.799
T-191	0.959	0.212	0.179	0.194	0.789
NMNH-2222	0.982	0.229	0.201	0.214	0.772
PO-1 Band	0.941	0.212	0.181	0.196	0.787
PO-1 Clear	0.941	0.212	0.181	0.196	0.788
P-386	0.904	0.228	0.196	0.213	0.771
P-195	0.950	0.220	0.187	0.202	0.779
P-344	0.935	0.216	0.185	0.200	0.784
NMNH-2345	1.007	0.196	0.174	0.185	0.804
NMNH-2343	0.983	0.178	0.155	0.166	0.822
NMNH-1396	0.991	0.185	0.160	0.172	0.815

Table 4. Fe^{57} Moessbauer Parameters from Selected Area Studies of Ortigas Site Specimen PO-1

Description	Linewidth Γ_L (mm/s)	Linewidth Γ_H (mm/s)	Intensity (L)	Intensity (H)	Quadrupole Splitting (mm/s)	Isomer Shift w.r.t. Fe (mm/s)
Clear with Collimator 1/4" x 1/16"	0.734	0.931	0.0721	0.0601	2.049	1.110
Band with Collimator 1/4" x 1/16"	0.729	0.927	0.0711	0.0593	2.052	1.109
Band with Collimator 2" x 1/25"	0.726	0.935	0.0349	0.0290	2.040	1.090

Table 5. Goodness-of-Fit Parameters for Two-Line Fits to Fe^{57} Moessbauer Spectra of Sample PO-1

Description	Chi Square χ^2	SIGNAL S	DISTANCE D	MISFIT (Per Cent)	Off-Resonance Counts/Channel
Clear with Collimator 1/4" x 1/16"	2059	2.19×10^5 $\pm 9.4 \times 10^2$	1.57×10^3 $\pm 8.2 \times 10^1$	0.72 ± 0.04	4.3×10^5
Band with Collimator 1/4" x 1/16"	2203	2.35×10^5 $\pm 9.7 \times 10^2$	1.72×10^3 $\pm 8.6 \times 10^1$	0.73 ± 0.04	4.8×10^5
Band with Collimator 2" x 1/25"	747	4.52×10^4 $\pm 4.3 \times 10^2$	2.60×10^2 $\pm 3.9 \times 10^1$	0.58 ± 0.09	4.0×10^5

Table 6a.

Fe^{57} Moessbauer Spectral Parameters of Basalt Glass at 298 K

	Quadrupole Interaction $e^2qQ/2$ (mm/sec)	Isomer Shift w.r.t. to Fe (mm/sec)	χ^2
Fe^{2+}	1.995±.001	1.0686±.001	3014
Fe^{3+}	0.575±.002	0.376±.004	

Table 6b.

Widths and Relative Intensities of Fe^{2+} and Fe^{3+} Fe^{57} Moessbauer Patterns of Basalt Glass at 298 K

	Γ_L (mm/sec)	Γ_H (mm/sec)	I_L (%)	I_H (%)	$\frac{\text{Area}(Fe^{3+})}{\text{Area}(Fe^{2+})}$	$\frac{Fe^{3+}}{Fe^{2+}}$ [a]
Fe^{3+}	0.430	0.624	0.01781	0.01228		
					0.126	0.257
Fe^{2+}	0.693	0.822	0.0877	0.07396		

[a] From wet chemical analysis

Table 7. Mössbauer Parameters of AN216 at 298 and 80°K Fitted with One and Two Quadrupole Doublets

	298°K		80°K	
	One	Two	One	Two
Γ_L (mm/sec)	0.751	0.584 0.585	0.847	0.666 0.718
Γ_H (mm/sec)	0.944	0.765 0.641	1.097	0.928 0.720
I_L	0.063	0.034 0.040	0.081	0.039 0.053
I_H	0.051	0.030 0.031	0.065	0.041 0.036
Isomer Shift w.r.t Fe (mm/sec)	1.063	1.084 1.029	1.202	1.227 1.160
Quadrupole Splitting (mm/sec)	1.927	2.275 1.572	2.105	2.518 1.757
χ^2	983	580	1918	888
MISFIT	0.38 ±0.04	0.0023 ±0.0007	0.35 ±0.02	0.0041 ±0.0005

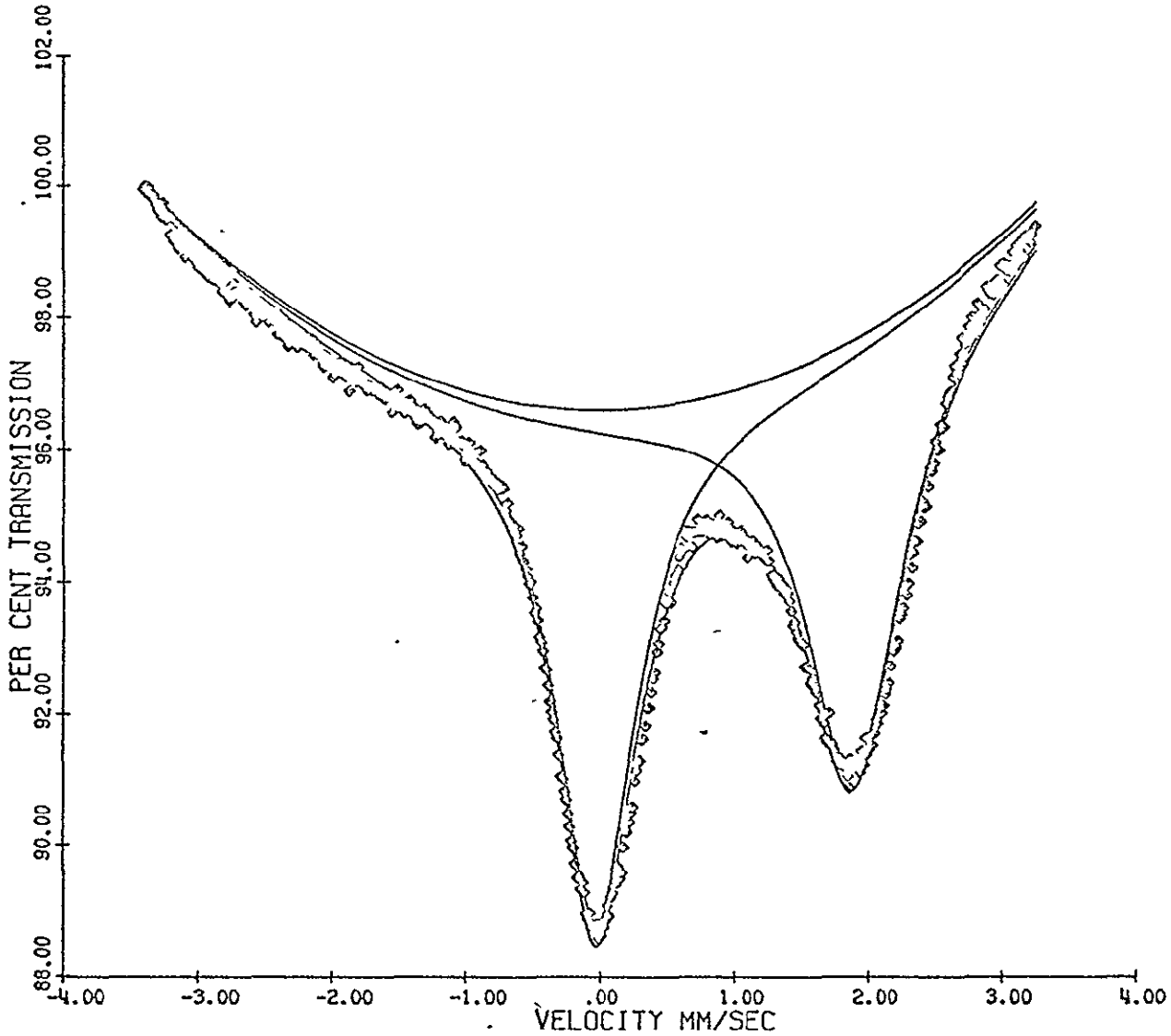

Fig. 1. Fe^{57} Moessbauer Spectrum of Normal Australite AN273 at 298°K

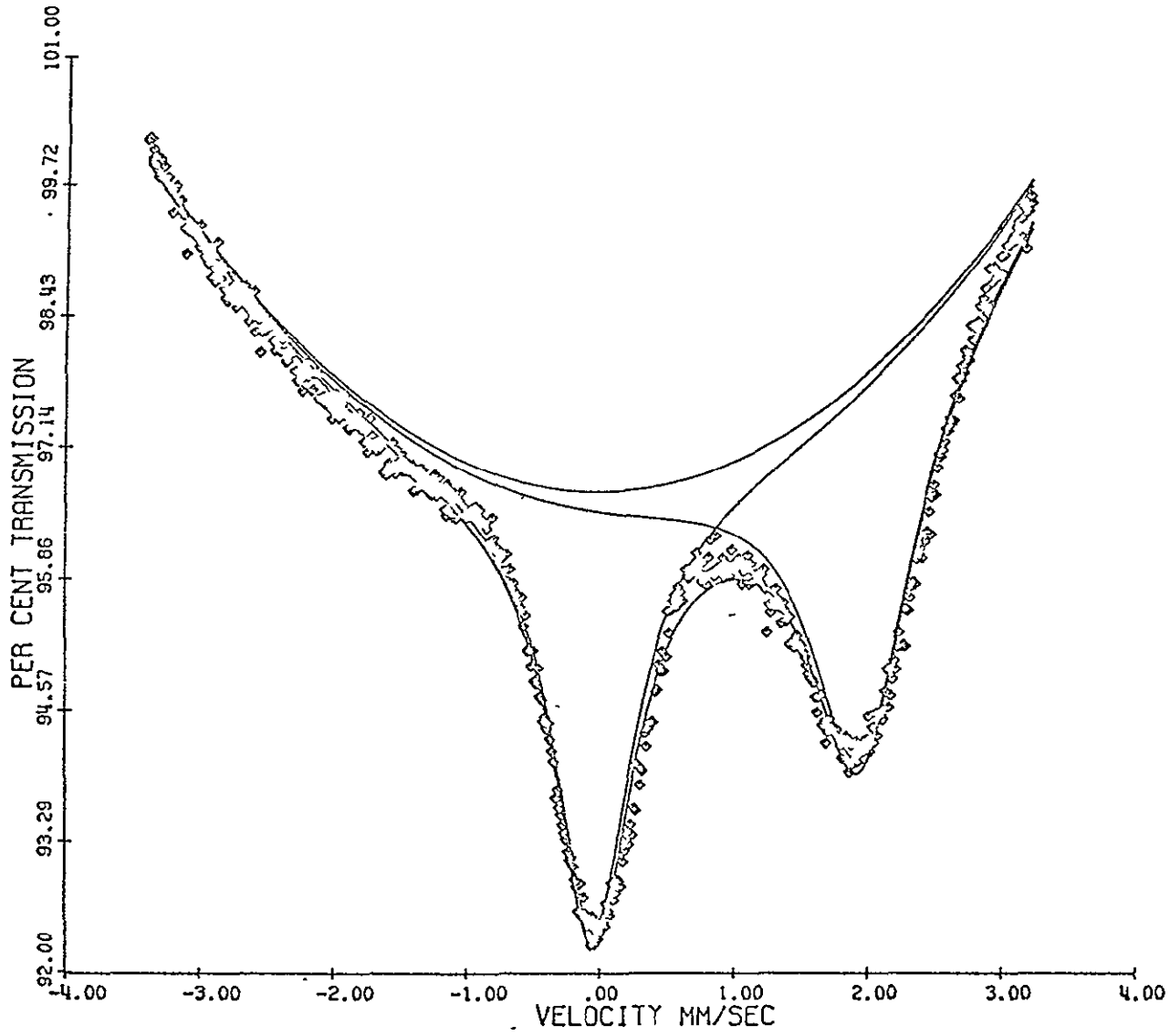

Fig. 2. Fe^{57} Moessbauer Spectrum of Philippinite P386 at 298°K

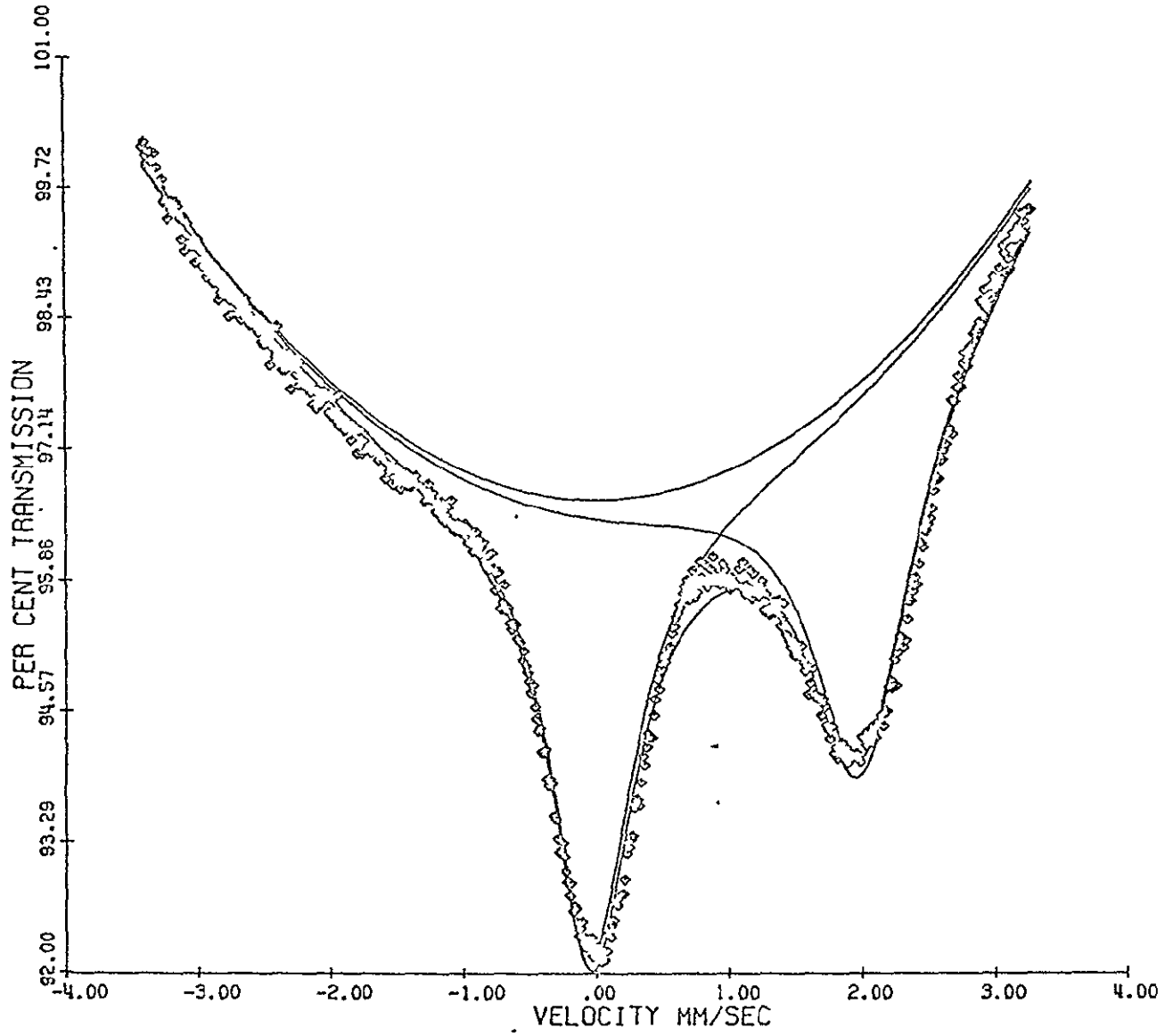

Fig. 3. Fe^{57} Moessbauer Spectrum of Georgia Tektite NMNH 1396 at 298 °K

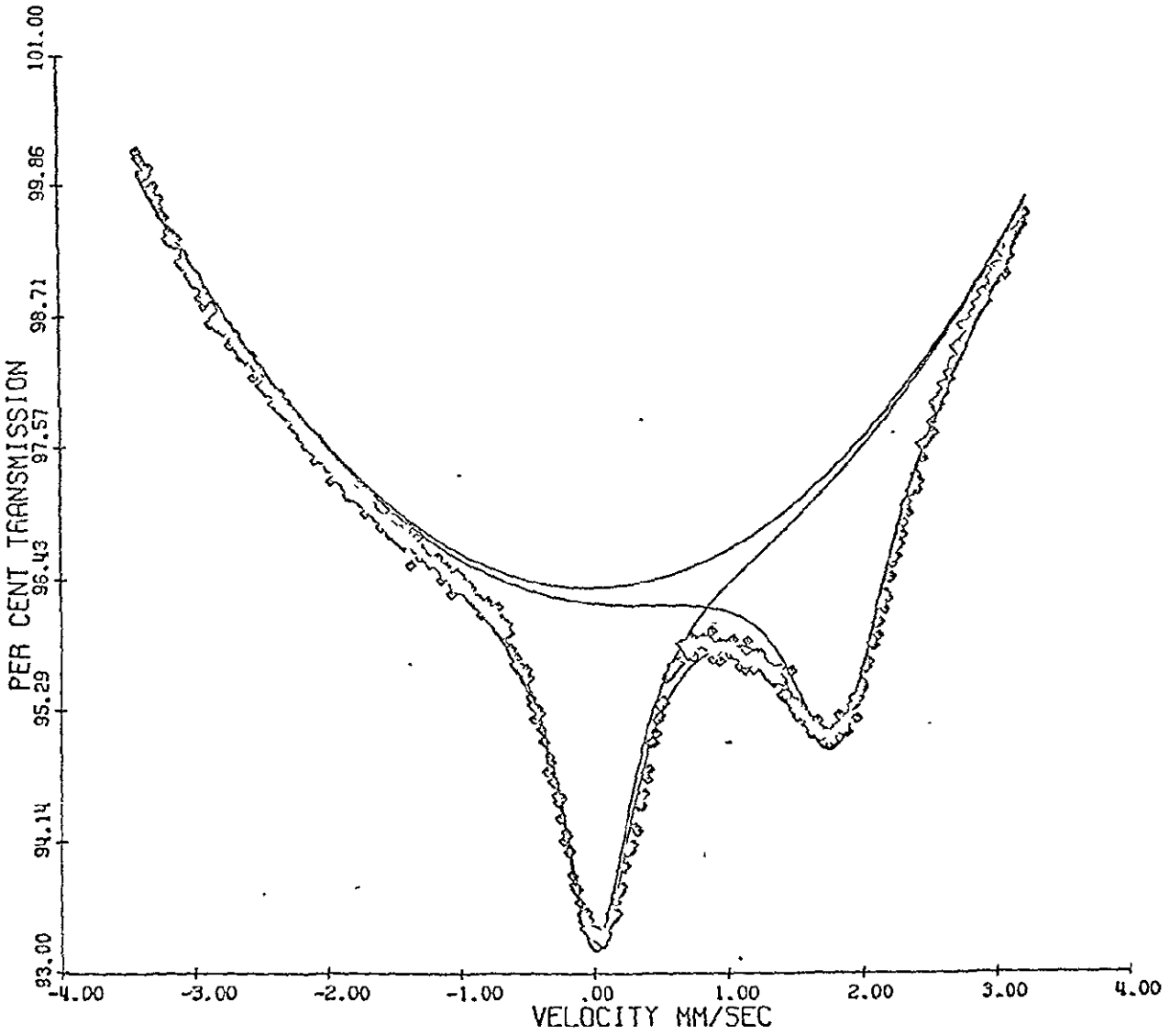

Fig. 4. Fe^{57} Moessbauer Spectrum of Moldavite NMNH 2230 at 298°K

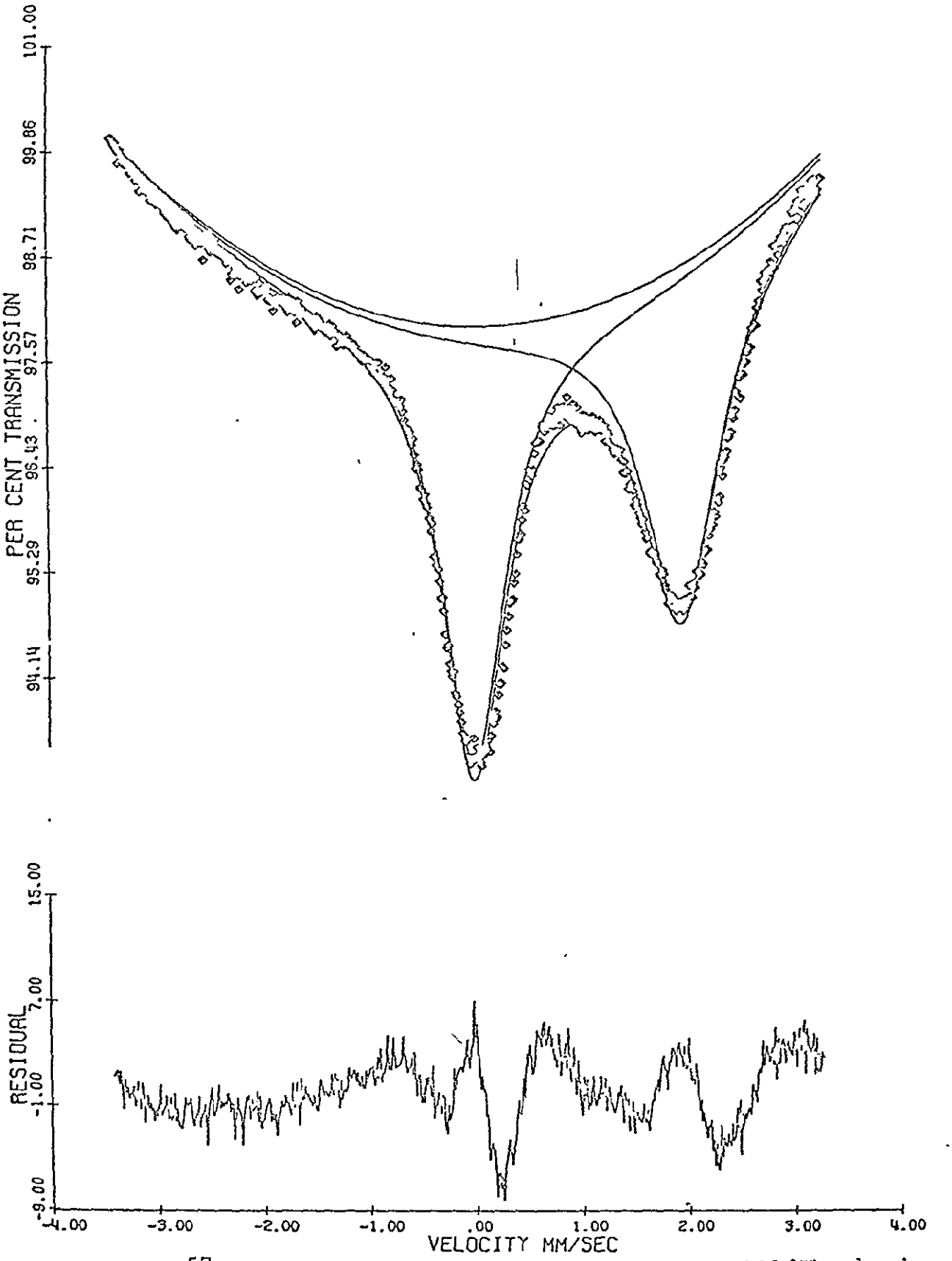

Fig. 5. Fe^{57} Moessbauer Spectrum of Indochinite I-43 at 298 °K, showing Fitted Spectrum(Solid Line) and RESIDUAL in Lower Half of Figure

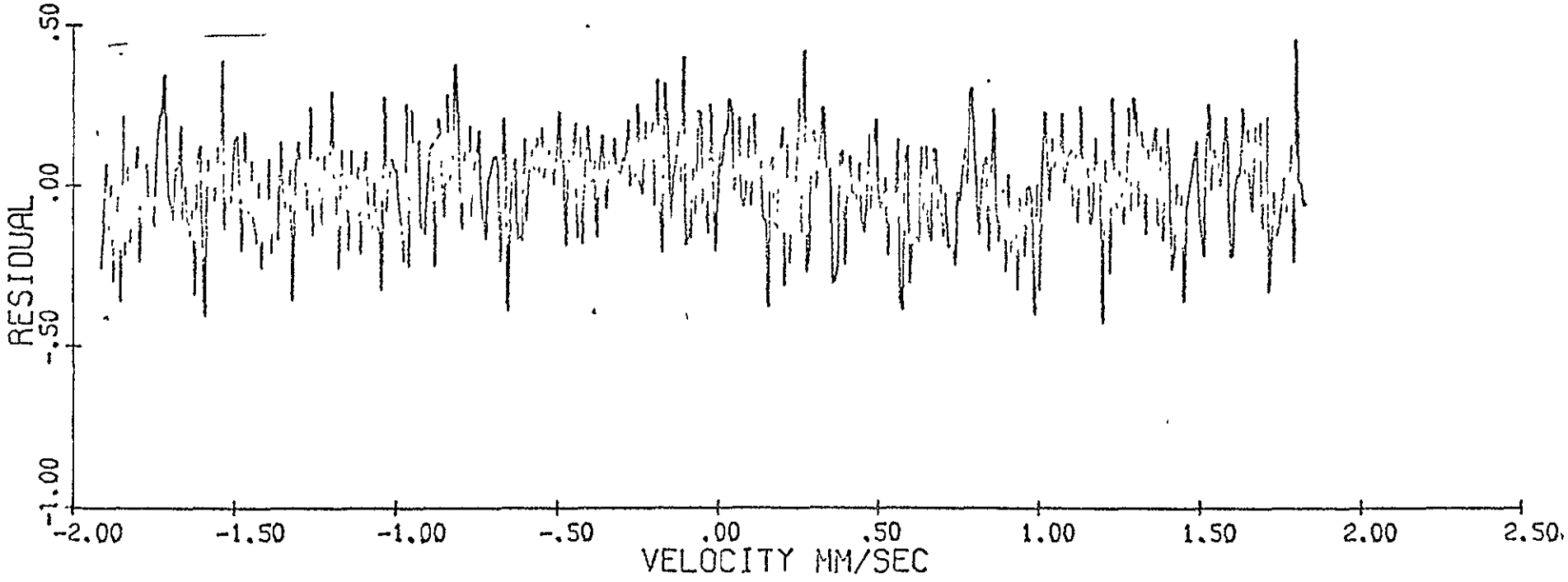

Fig. 6. "Grass-Like" Appearance Expected for RESIDUAL When Fit to a Spectrum is Adequate

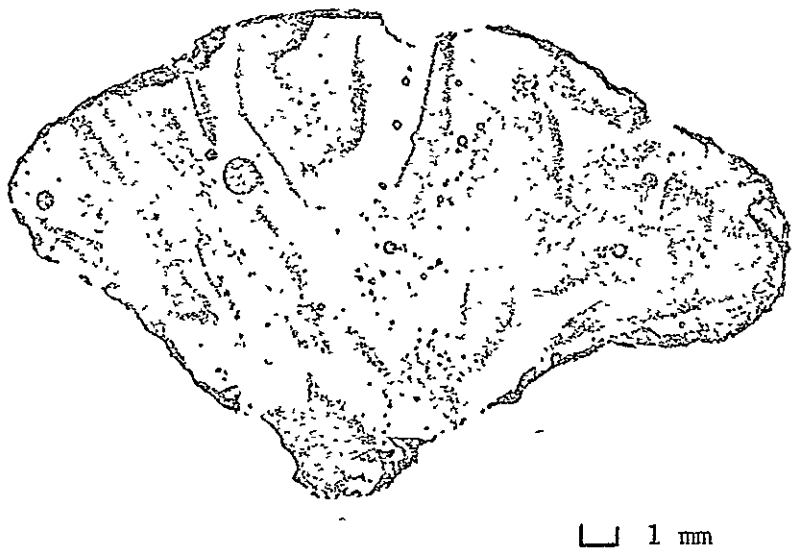

Fig. 7. A thin section of an Ortigas site Tektite (PO-1) showing band-like patterns

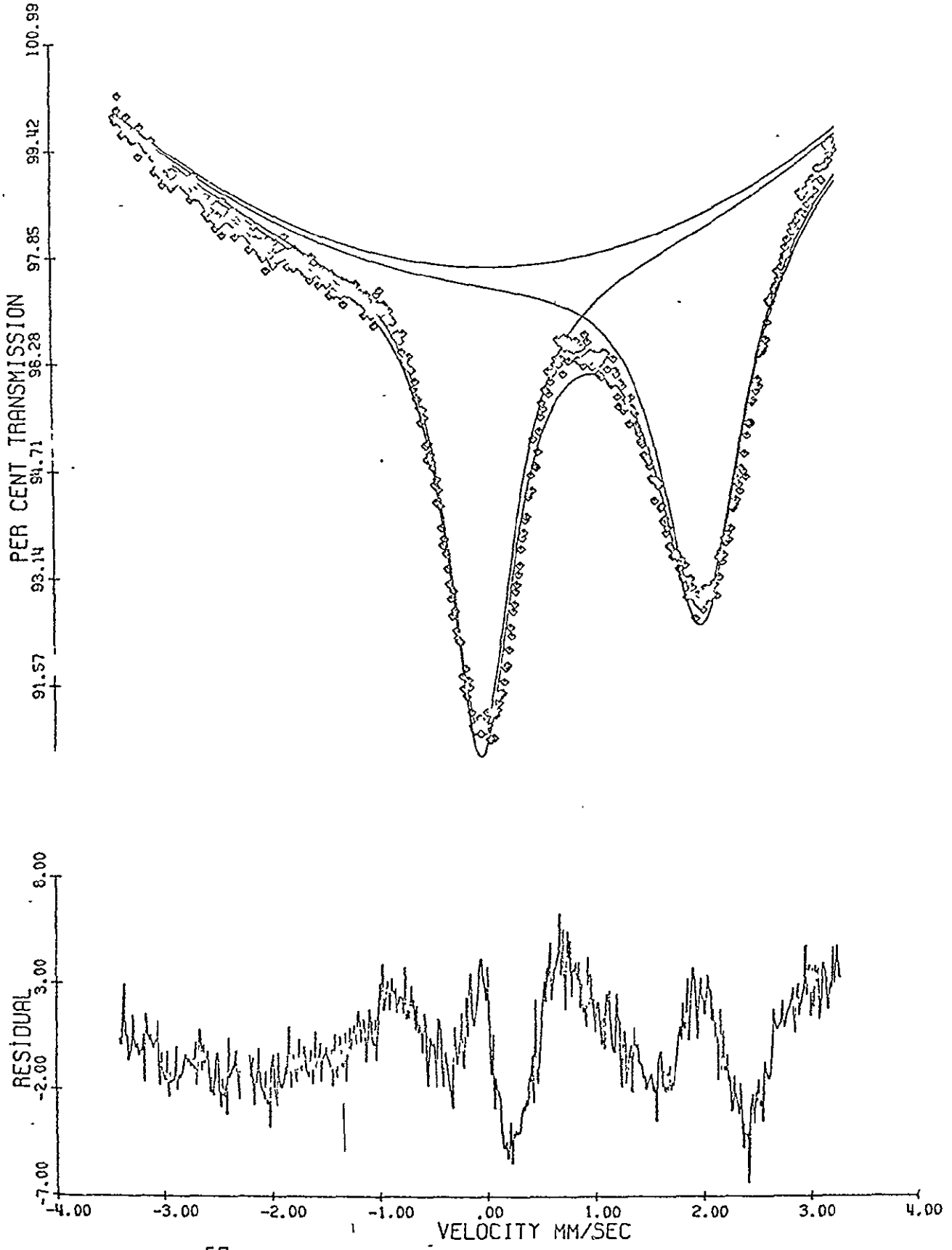

Fig. 8. Fe^{57} Moessbauer Spectrum at 298°K of Dark Band of Ortigas Site Philippinite obtained Using Short Collimator, Note Similarity of Structure in RESIDUAL to That in Fig. 12.

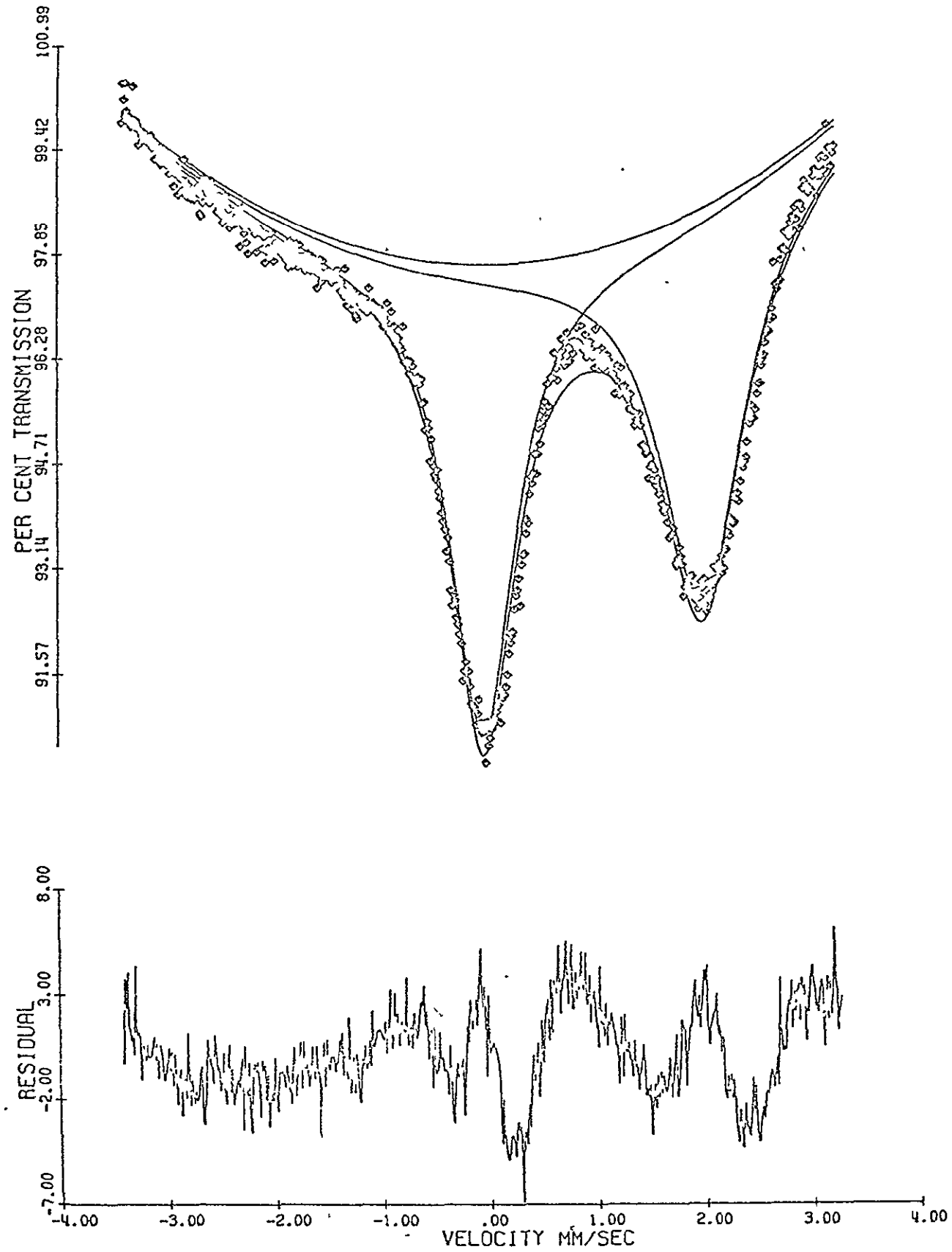

Fig. 9. Fe^{57} Moessbauer Spectrum at 298°K of Clear Region of Ortigas Site Philippinite Obtained Using the Short Collimator. Note Similarity of Structure in RESIDUAL to That in Fig. 11.

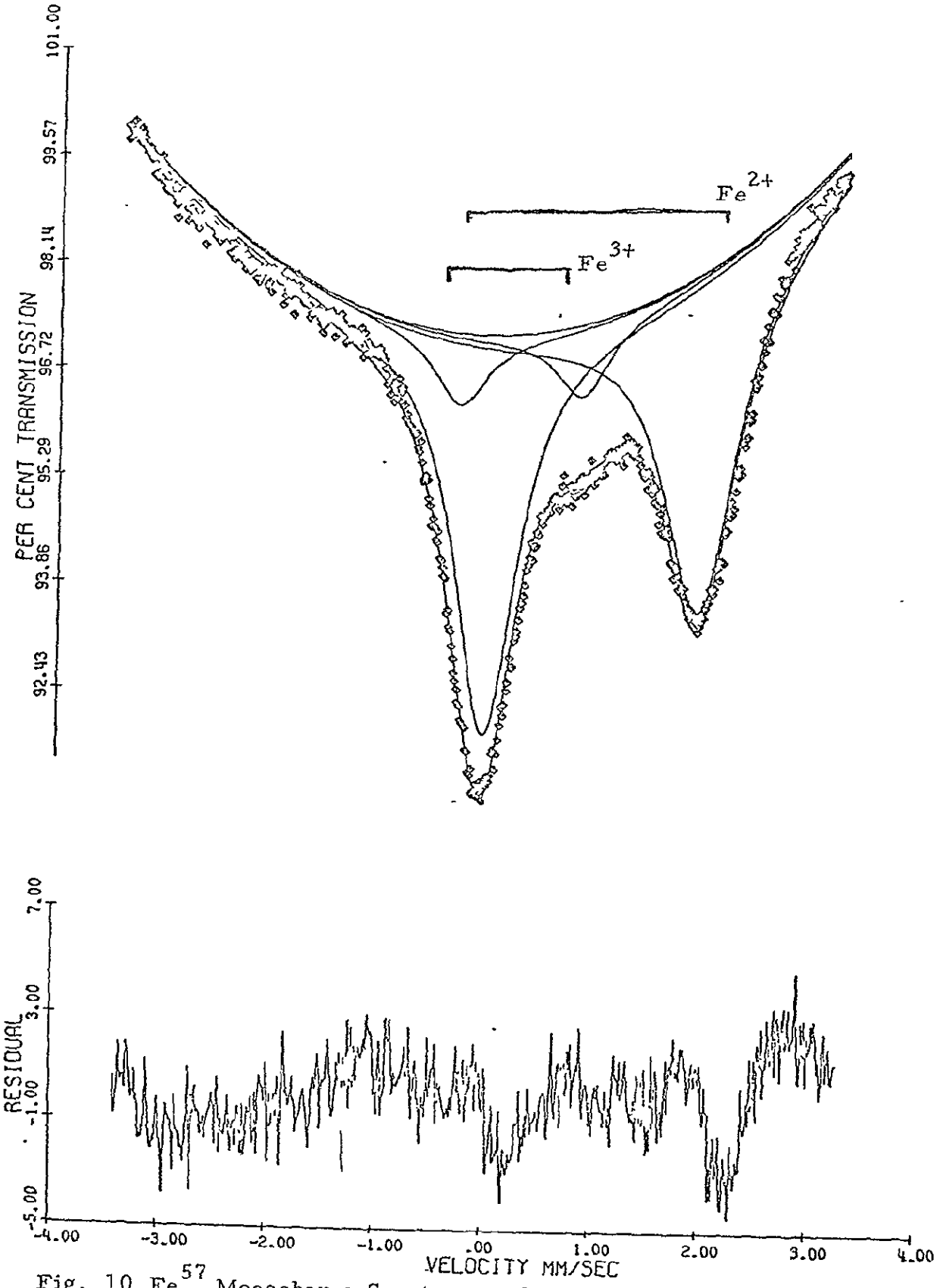

Fig. 10. Fe^{57} Moessbauer Spectrum at 298°K of Synthetic Basalt Glass Containing Fe^{2+} and Fe^{3+} Ions. Fe^{3+}/Fe^{2+} =0.1.

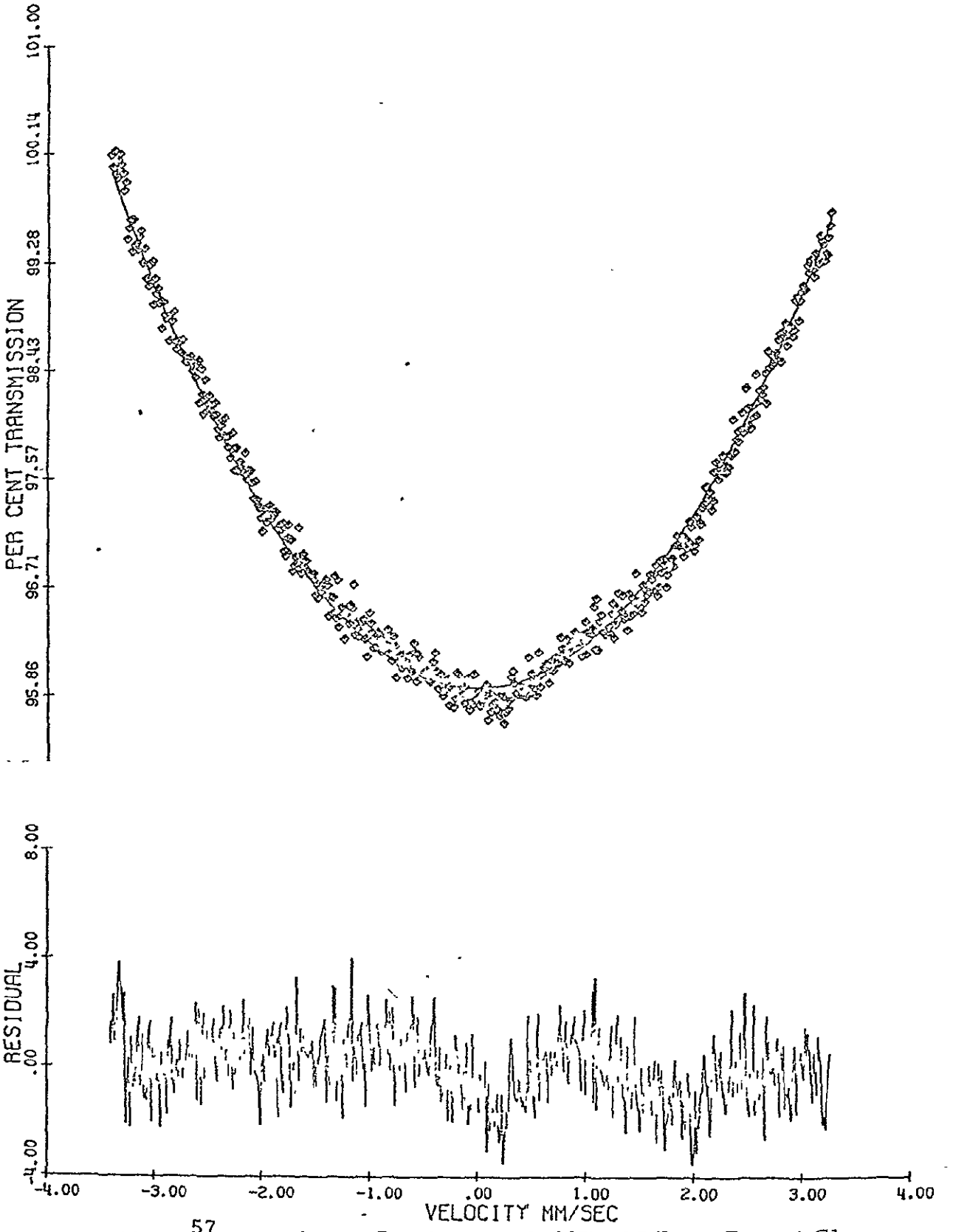

Fig. 11. Fe^{57} Moessbauer Spectrum at 298°K of Libyan Desert Glass NMNH 1212. Note Similarity of Structure in RESIDUAL to Typical Tektite Spectrum.

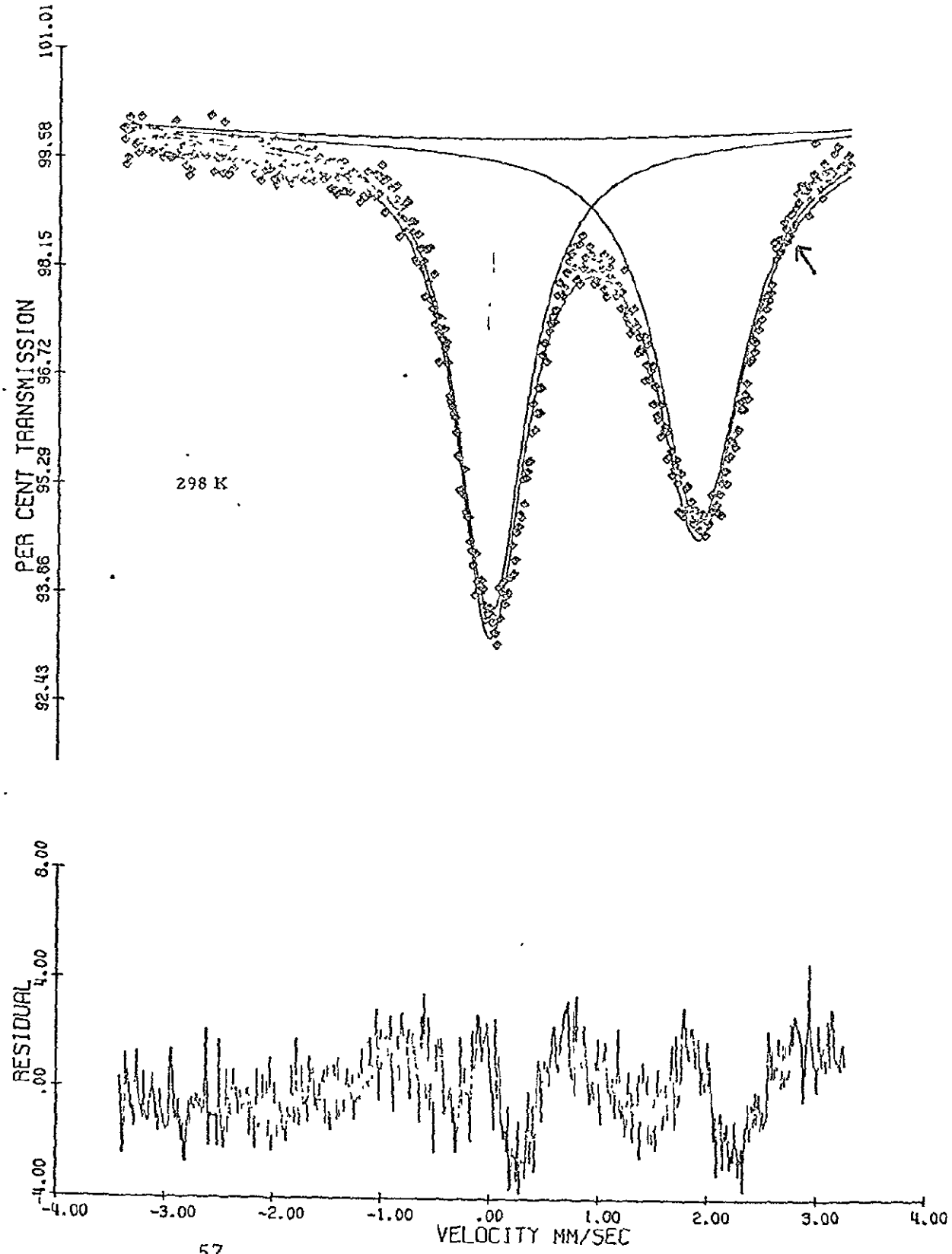

Fig. 12. Fe^{57} Moessbauer Spectrum at 298°K of HCa Australite AN216. Note Weak Shoulder Indicated by Arrow.

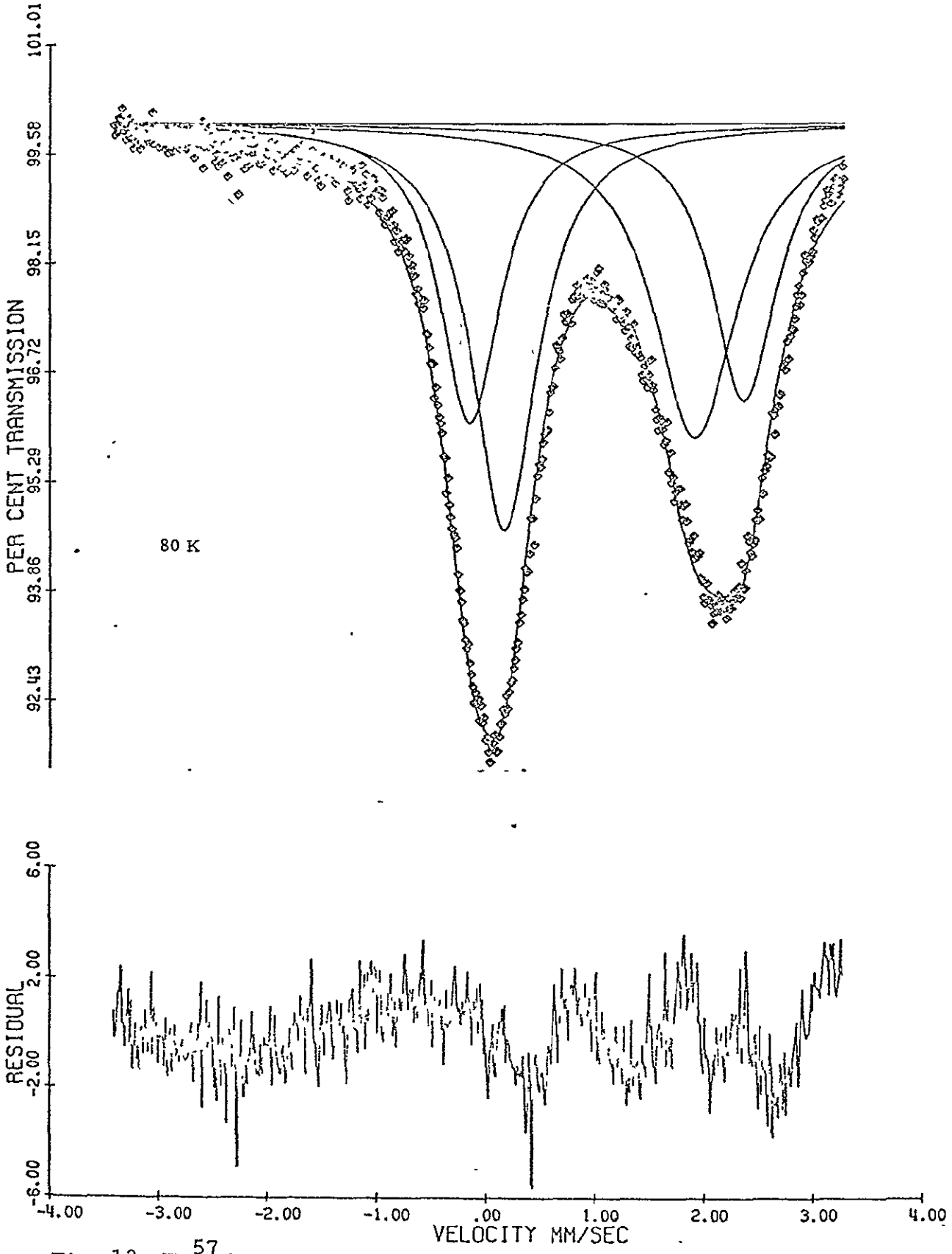

Fig. 13. Fe^{57} Moessbauer Spectrum at 77°K of HCa Australite AN216, Showing Results of Fitting Two Quadrupole Doublets. Note Weak Structure in RESIDUAL.

Table 8. Mössbauer Parameters at 298°K of Crystalline Bronzite and Clinopyroxene

A. SINGLE QUADRUPOLE DOUBLET FIT

	Quadrupole Interaction (mm/sec)	Isomer Shift (mm/sec)	$\frac{\text{Area}_{\text{Low}}}{\text{Area}_{\text{High}}}$	MISFIT (%)
Bronzite	2.161	1.166	1.140	0.4 ± .02
Clinopyroxene	2.110	1.179	1.02	0.3 ± .01

B. TWO QUADRUPOLE DOUBLET FIT

		Quadrupole Interaction (mm/sec)	Isomer Shift (mm/sec)	A(1)/A(2)	MISFIT (%)
Bronzite	1	2.412	1.173	.13	0.2 ± .01
	2	2.118	1.169		
Clinopyroxene	1	2.234	1.201	1.87	0.002 ± .0002
	2	1.971	1.165		

C. THREE QUADRUPOLE DOUBLET FIT

		Quadrupole Interaction (mm/sec)	Isomer Shift (mm/sec)	Relative Intensity	MISFIT (%)
Clinopyroxene	1	2.624	1.200	18	.05 ± .01
	2	2.221	1.215	20	.05 ± .01
	3	1.964	1.187	62	.05 ± .01

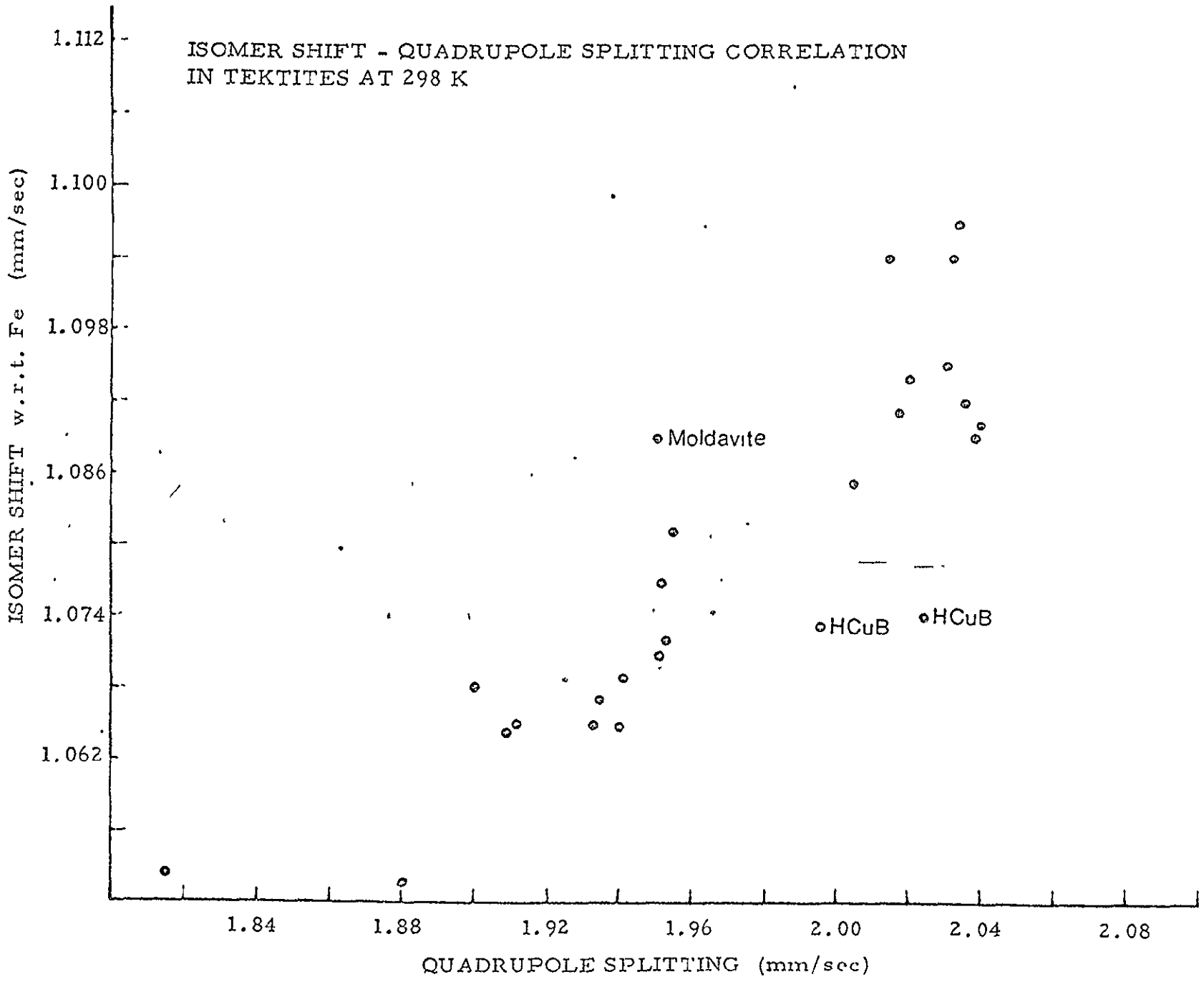
ISOMER SHIFT - QUADRUPOLE SPLITTING CORRELATION
IN TEKTITES AT 298 K
ISOMER SHIFT w.r.t. Fe (mm/sec)
1.112
1.100
1.098
1.086
1.074
1.062
Moldavite
HCuB
HCuB
1.84
1.88
1.92
1.96
2.00
2.04
2.08
QUADRUPOLE SPLITTING (mm/sec)

Fig. 14.

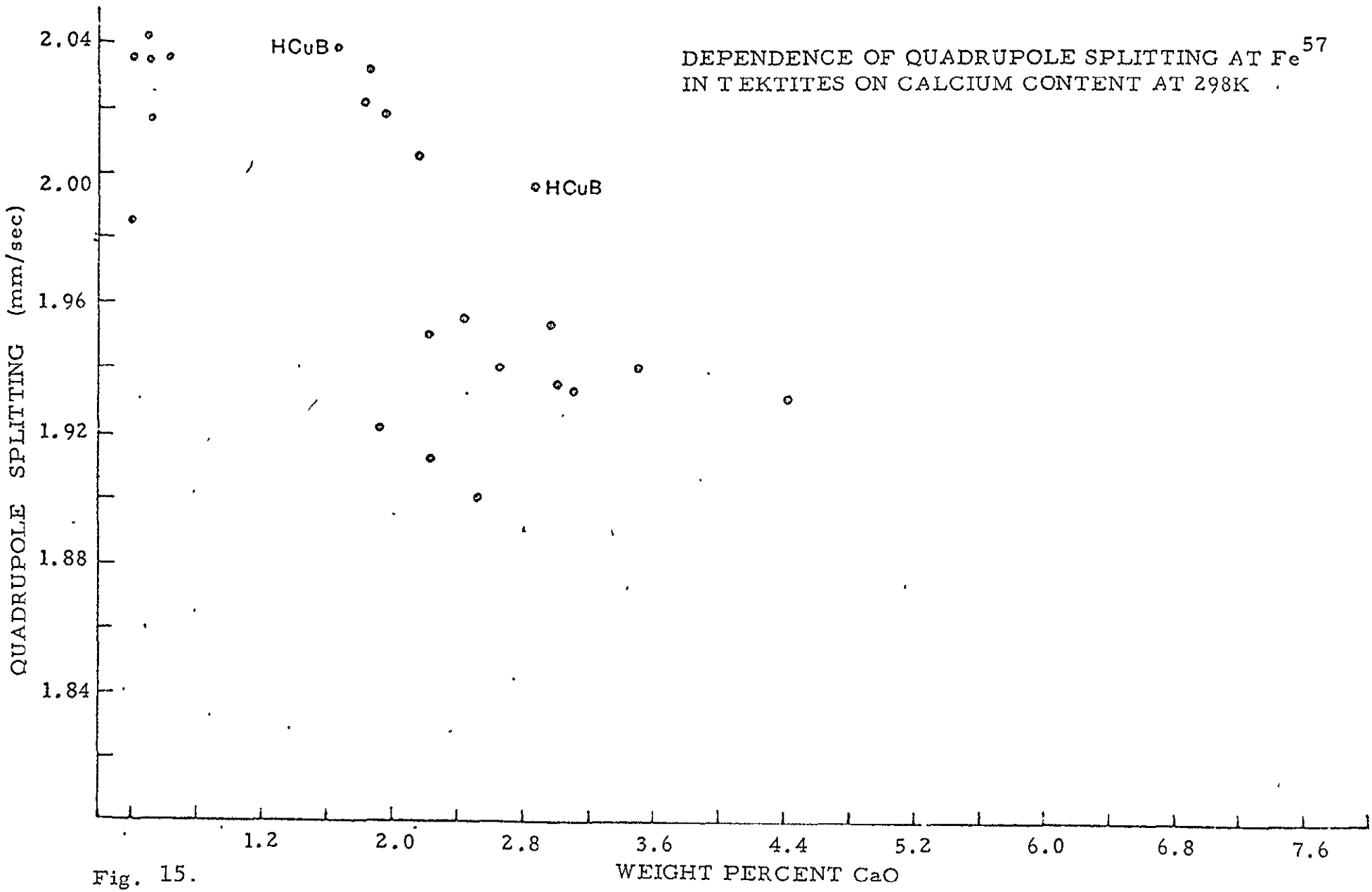
DEPENDENCE OF QUADRUPOLE SPLITTING AT Fe^{57}
IN TEKTITES ON CALCIUM CONTENT AT 298K
HCuB
HCuB
QUADRUPOLE SPLITTING (mm/sec)
2.04
2.00
1.96
1.92
1.88
1.84
1.2
2.0
2.8
3.6
4.4
5.2
6.0
6.8
7.6
WEIGHT PERCENT CaO

Fig. 15.

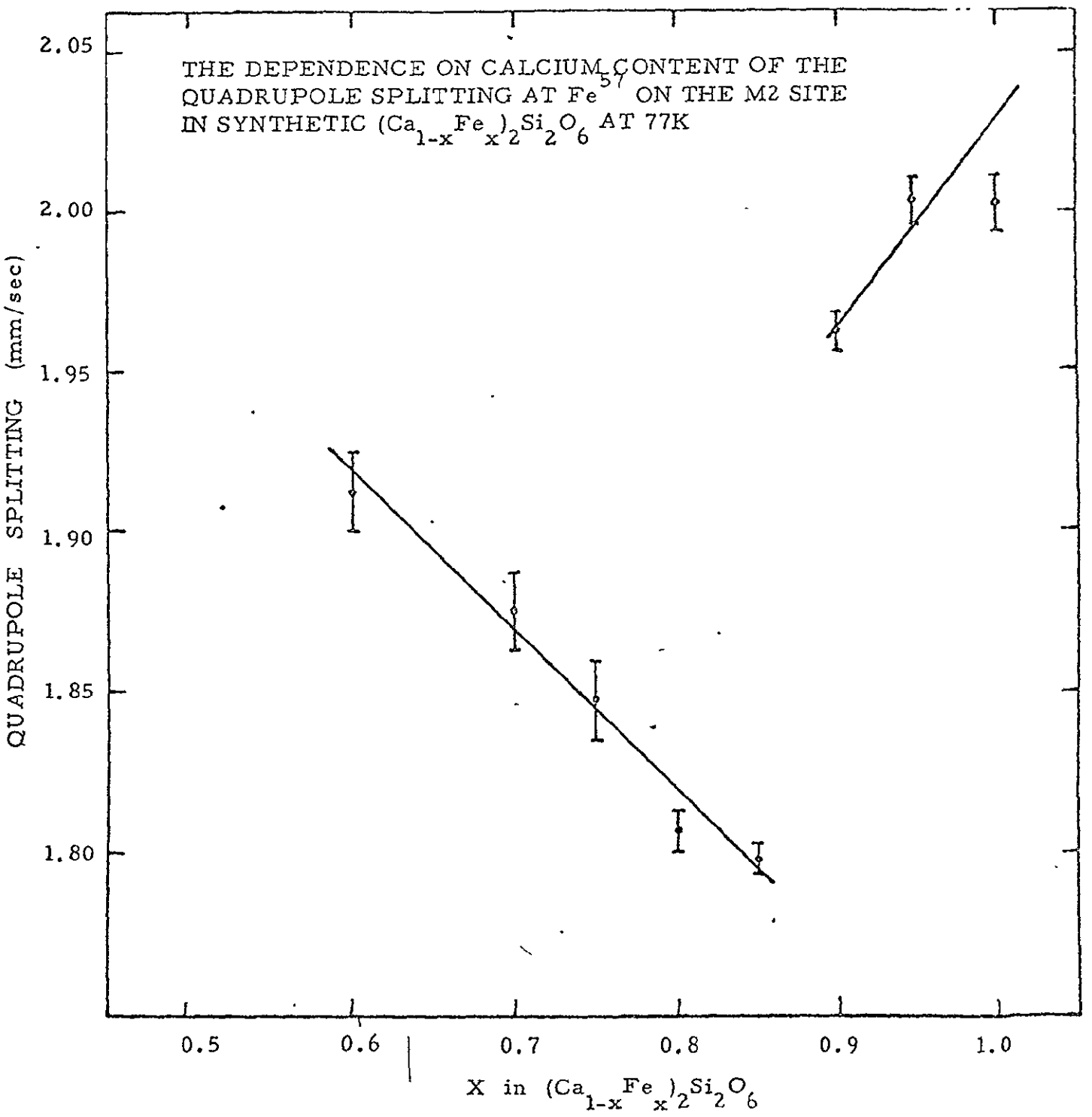

Fig. 16A.

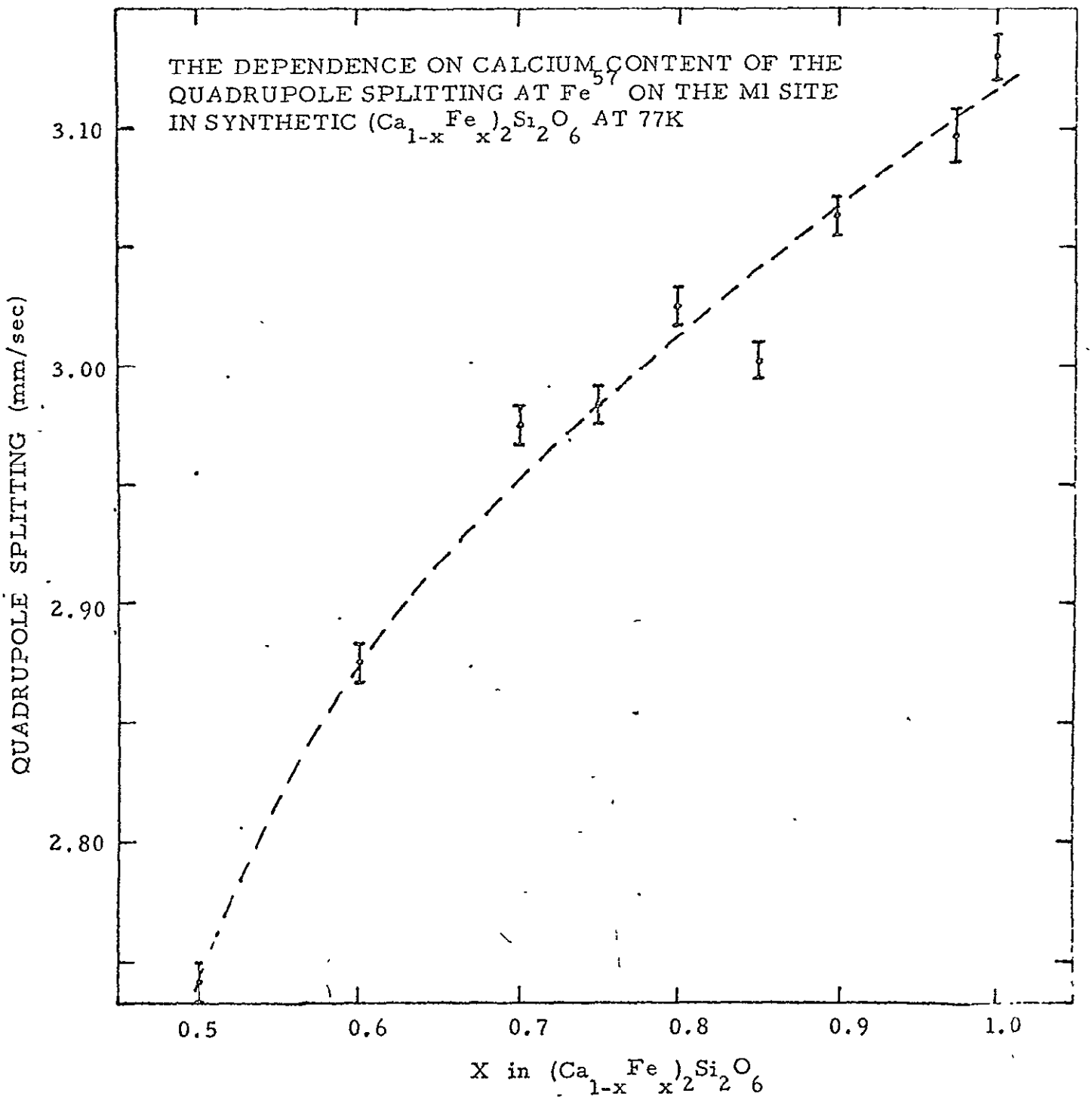
THE DEPENDENCE ON CALCIUM CONTENT OF THE QUADRUPOLE SPLITTING AT Fe^{57} ON THE M1 SITE IN SYNTHETIC $(Ca_{1-x}Fe_x)_2Si_2O_6$ AT 77K
QUADRUPOLE SPLITTING (mm/sec)
3.10
3.00
2.90
2.80
0.5
0.6
0.7
0.8
0.9
1.0
X in $(Ca_{1-x}Fe_x)_2Si_2O_6$

Fig. 16B.

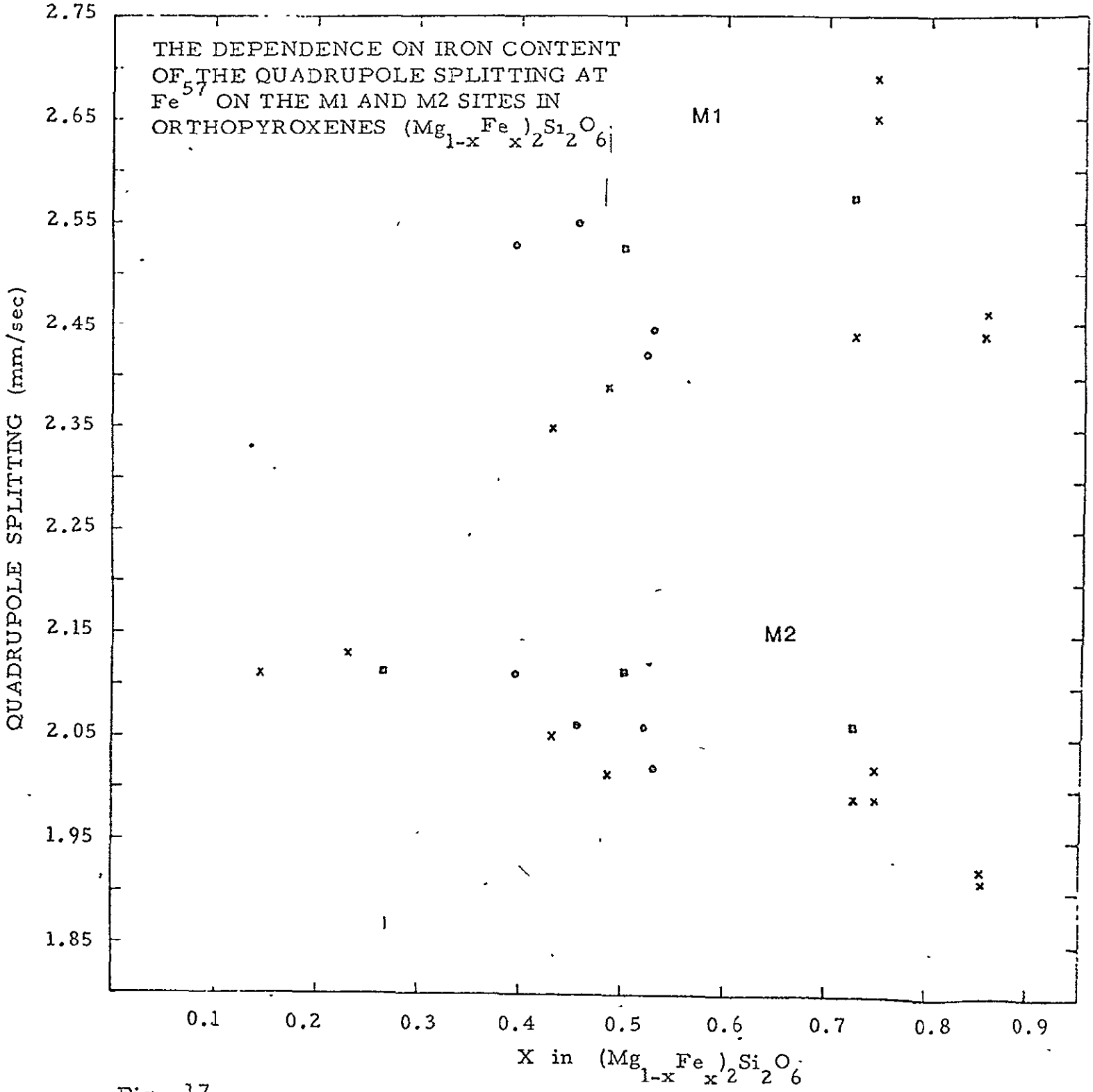
THE DEPENDENCE ON IRON CONTENT OF THE QUADRUPOLE SPLITTING AT Fe^{57} ON THE M1 AND M2 SITES IN ORTHOPYROXENES $(Mg_{1-x}Fe_x)_2Si_2O_6$
M1
M2
QUADRUPOLE SPLITTING (mm/sec)
2.75
2.65
2.55
2.45
2.35
2.25
2.15
2.05
1.95
1.85
0.1
0.2
0.3
0.4
0.5
0.6
0.7
0.8
0.9
X in $(Mg_{1-x}Fe_x)_2Si_2O_6$

Fig. 17.

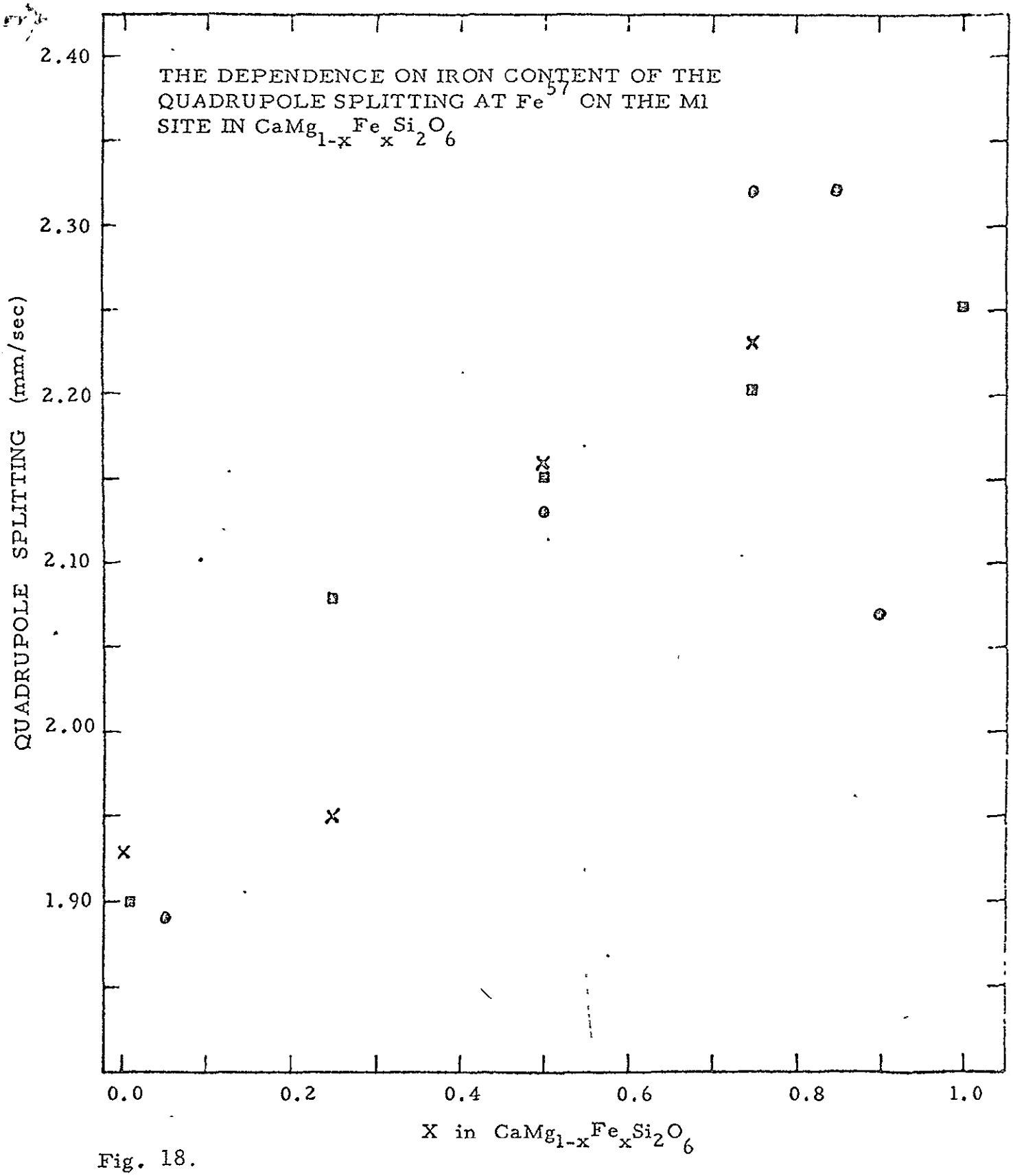

Fig. 18.